

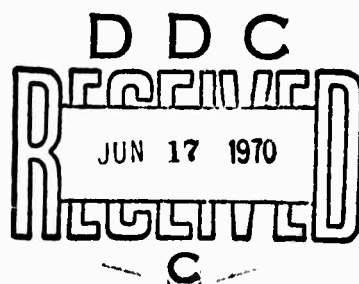
RESEARCH PAPER P-581

DETECTION CONSIDERATIONS FOR LASER SYSTEMS
IN THE NEAR INFRARED:
PROGNOSIS FOR AN IMPROVED TECHNOLOGY

AD707317

A. Fenner Milton
Alvin D. Schnitzler

April 1970



INSTITUTE FOR DEFENSE ANALYSES
SCIENCE AND TECHNOLOGY DIVISION

This document has been approved
for public release and sale; its
distribution is unlimited.

IDA Log No. HQ 70-10983
Copy 94 of 150 copies

ACCESSION NO.		
CPSTI	WHITE SECTION	<input checked="" type="checkbox"/>
DOC	BUFF SECTION	<input type="checkbox"/>
UNANNOUNCED		<input type="checkbox"/>
JUSTIFICATION		
BY		
DISTRIBUTION/AVAILABILITY CODES		
DIST.	AVAIL. GRD.	SPECIAL
1		

The publication of this IDA Research Paper does not indicate endorsement by the Department of Defense, nor should the contents be construed as reflecting the official position of that agency.

This document has been approved for public release and sale; its distribution is unlimited.

RESEARCH PAPER P-581

DETECTION CONSIDERATIONS FOR LASER SYSTEMS
IN THE NEAR INFRARED:
PROGNOSIS FOR AN IMPROVED TECHNOLOGY

A. Fenner Milton
Alvin D. Schnitzler

April 1970



INSTITUTE FOR DEFENSE ANALYSES
SCIENCE AND TECHNOLOGY DIVISION
400 Army-Navy Drive, Arlington, Virginia 22202

Contract DAHC15 67 C 0011
ARPA Assignment 5

PREFACE

This report is designed specifically for those physicists who are concerned with near-infrared detection. Its intent is to illustrate how possible improvements in detector materials and devices can influence the near-infrared systems of most interest to the military.

Most of the material for this report was collected in connection with the study on optically pumped lasers that was conducted at the Institute for Defense Analyses during the fall of 1969. The results of that study will be found in IDA Research Paper P-547, Report of the Study on Optically Pumped Lasers and Nonlinear Optics, by J. L. Walsh, J. F. Asmus, and A. F. Milton.

ACKNOWLEDGMENT

We would like to thank the many members of the detector community who have supplied the information which made this report possible.

ABSTRACT

This paper summarizes the influence of detection considerations on the standard military optically pumped laser systems. The problems and uncertainties associated with the development of new photocathodes for the near infrared are discussed in detail. A variety of laser detection schemes are examined to determine their potential in the $\lambda = 1.5\mu$ to 2.5μ region. The problems of imaging systems for use with laser illuminators are discussed. A research program is recommended to improve detector performance.

CONTENTS

I. Introduction	1
II. Systems Considerations and Detector Requirements	2
III. Photocathodes	8
IV. Avalanche Diodes	24
V. Avalanche in III-V Compounds	26
VI. Large-Area Diodes	27
VII. Photoconductors and AC Bias	29
VIII. Heterodyne	31
IX. Amplification and Upconversion	31
X. Laser Imaging Systems	36
XI. Recommendations	43
XII. Overview: Detectors for Laser Applications	45
References	48

TABLES

1. Detector Noise Equivalent Power	10
2. Photocathode Characteristics	13

FIGURES

1. Heterojunction Energy-Level Diagram for GaAs-Cs ₂ O. $\Delta\chi$ is the difference in electron affinities of the two materials.	15
2. Photon Induced Tunnel Emitter	22
3. Passive Performance of Triple Image Intensifier	39

I. INTRODUCTION

The majority of laser systems use the laser to elicit or to transmit information and therefore require a detection subsystem. In the military sphere, the important rangefinder, target-designator, illuminator, and line-scan systems all require detectors, and improvements in detector sensitivity would be as useful in these systems as higher laser pulse energies. Laser requirements based upon the present state of the detector art could be relaxed if detector improvements were forthcoming. Systems improvements (longer range, for example) can be obtained with higher power lasers or with more sensitive detectors.

However, two considerations make improvements in detector sensitivity particularly attractive:

1. Unless it is practical to operate at eye-safe wavelengths ($\lambda > 1.5\mu$), higher pulse energies increase the eye-damage problem whereas improvements in detector sensitivity do not. For laser systems in which $\lambda > 1.5\mu$, the eye-damage threshold is above 0.1 joule/cm^2 instead of the 10^{-6} to $10^{-7} \text{ joule/cm}^2$ at $\lambda = 1.06\mu$ (Q switched). Unfortunately, neither solid-state lasers nor detectors operate as efficiently at eye-safe wavelengths.
2. Higher pulse energies are usually obtained with heavier systems, which, even if successful, require more input power and heavier power supplies. Some increase in efficiency, but not enough to compensate, can be obtained by working far above threshold.

Unless extensive cooling is necessary, detector improvements usually do not require increased weight and power. Thus promising avenues for detector research and development deserve attention.

II. SYSTEMS CONSIDERATIONS AND DETECTOR REQUIREMENTS

Low-duty-cycle direct detection systems (not signal-shot-noise-limited or heterodyne systems) detect peak power so that for a given pulse energy short pulses are, in principle, easier to detect.

$$P_{\min}(\Delta\tau) \sim (\Delta\tau)^{1/2} \quad (1)$$

where P_{\min} = minimum signal power for $S/N = 1$ and $\Delta\tau$ = pulse length. This will not be true for imaging systems which must integrate the flux over a frame time, and detection improvements can be gained by shortening the pulse only if the detector can resolve the pulse without losing sensitivity. For the most important types of detectors, this speed is ultimately limited by electron transit time effects, which become important at about $f = 2$ to 5 GHz, $\Delta\tau = 0.5$ to 0.2 nsec for state-of-the-art diodes and photocathodes (Ref. 1).

The quantum nature of the return signal is important and does enter in for short pulses with low-noise detectors. For reasonable detection more than two photons have to be detected during the return so that

$$P_{\min} > \frac{2hc}{\eta\lambda\Delta\tau} \quad (2)$$

where η is the detector quantum efficiency. This corresponds to a signal-shot-noise-limited voltage signal-to-noise ratio of $\sqrt{2}$. Pulse lengths that would give P_{\min} less than this (following Eq. 1) do not offer improvements, since in this regime of few return photons even a direct detection system counts photons and does not measure peak power. For the wavelengths of paramount interest this crossover usually occurs for pulse lengths shorter than 10 nsec. However, fluctuations in the signal can become important with longer pulses for larger signal-to-noise ratios and favorable detection conditions.

There are other considerations when choosing a pulse length. For imaging systems there is a desire to reject backscatter, as from fog, or to see past a bright light. Except for silhouette viewing, short pulses are necessary, since for clarity the return from the target must not coincide in time with the return from the fog. The range of coincidence is $\Delta\tau c/2$, which is 150 m for a 1- μ sec pulse. Since an imaging system probably should not have its range of view restricted any more, shorter pulses are probably unnecessary for range gating. For a point detector which resolves the return pulse, this type of gating can be done in the electronics, but an imaging system must actually turn the detector off.

Resolving a short pulse without losing sensitivity requires very large detector gains to avoid the Johnson noise problems caused by the necessarily small value of the load resistor. Exactly what gain is required depends on the leakage current of the detector, on the background conditions, and on the multiplication noise characteristics. A practical example for a small detector, free of excess noise, shows that gains larger than $500/\eta^{1/2}$ (η = quantum efficiency) are necessary for background-limited operation with $\Delta\tau < 10$ nsec. Since gains larger than $1000/\eta^{1/2}$ are not easily obtainable, there is no advantage as yet, from a detection point of view, in seeking pulses shorter than 10 nsec. Detectors having a larger field of view (FOV) will have more dark current and, in that case, shorter pulses may be advantageous with available gains.

A rangefinder benefits from short pulses in that it can range more accurately. For a single pulse

$$\delta R = \frac{c \Delta\tau}{\sqrt{(S/N)_p}} \quad (3)$$

which means that a 10-nsec pulse with $S/N = 1$ can range to within 3 m, which is certainly accurate enough for military applications.

The main conclusion to be drawn from the above is that the 10- to 30-nsec Q-switched pulse (easily formed with an optically pumped solid-state laser) is well suited for most military detection problems.

However, longer pulses up to 1 μ sec would be satisfactory for gated imaging systems, and somewhat shorter pulses may be useful if large-FOV detectors are required. Line-scan systems, of course, use cw operation.

In the visible and near infrared optically pumped laser systems offer some choice of principal laser wavelength:

0.694 μ	Ruby (visible)	
1.06 μ	Nd ³⁺ YAG, glass (YAG more efficient)	
1.54 μ	Er ³⁺ glass	} (eye-safe)
1.61 μ	Er ³⁺ LaF ₃	
1.65 μ	Er ³⁺ YAG	
2.1 μ	Ho ³⁺ YAG	

Cooled gallium arsenide laser diodes emit at 0.86 μ . Since laser pulse detectors are usually photon detectors, one would normally think that detection would be made easier by going to longer wavelengths where there are more photons per watt. However, such is not the case. Better detectors are easier to fabricate for high-energy photons.

In the overall system, background and transmittance (for a modal clear standard atmosphere) characteristics are important and should be compared (Ref. 2). Target contrast can improve at longer wavelengths.

Wavelength, microns	<u>0.69</u>	<u>1.06</u>	<u>1.54</u>	<u>2.1</u>
Attenuation coefficient, per km	0.15	0.12	0.1	0.09
Background radiance (sunlit surface), w/cm ² sterad Å	3x10 ⁻⁶	1.5x10 ⁻⁶	0.5x10 ⁻⁶	0.2x10 ⁻⁶

This shows that improvements can be made in both transmittance and daytime sunlit background levels by moving towards longer wavelengths, but that these improvements are not dramatic (Ref. 2). These values are highly dependent on weather, atmospheric conditions, and time of day. Moonlight background levels are a factor of 10⁶ less. The importance of background radiation depends on the width of the spectral filter that can be used, which will ultimately be limited by the stability of

the laser. A practical lower limit for systems having a small FOV seems to be 20\AA . Even this may be too small for 1.06μ and 1.54μ .

Rangefinders (typically 0.2 pulse/sec) need small-FOV point detectors (FOV < 5 milliradians) that can resolve 10- to 30-nsec pulses. The detector area need not be very large. For example, with an objective of 6-cm diameter and f:2 optics, a detector 600μ (25 mil) in diameter gives a 5-milliradian FOV. Cooling is inconvenient in man-carried rangefinder systems.

Target designators (typically 10 pulses/sec) need detectors with a larger FOV. A quadrant with a total FOV of 24 deg ($\sim 1/2$ radian) is often used (Ref. 3). Short pulses can be resolved, but the total detector needs to be at least a centimeter in diameter. The total background on these detectors will be a factor of 10^4 higher than on smaller-FOV detectors. This background will be very significant in sunlit situations. Since these detectors are throwaway systems, low cost and lack of a cooling requirement are important.

Illuminators (typically 30 pulses/sec) need a 1- to 5-deg imaging system (the only advantage in using a laser instead of a searchlight involves range gating or a relatively small FOV) that can be range gated at the detector. This implies, of course, imaging detection systems for sensitivity or film for higher resolution. There is some interest in very-long-range imaging (in the visible where more sensitive film is available) with milliradian FOVs at lower repetition rates.

Line-scan systems operating CW need small-FOV point detectors and good response to signal frequencies up to a maximum of 15 MHz ($1/2$ -radian total FOV, $1/2$ -milliradian beam, $1/30$ -sec frame time). With CW operation geometrical techniques can be used to reject backscatter originating near the transmitter. Range gated pulses are not appropriate since the easy comparison of one resolution element to the next would be lost. Laser amplitude stability of 1 percent (difficult for solid-state lasers) is required.

In the near infrared there are two principal types of detectors: photoemissive cathodes and diodes (avalanche or nonavalanche).

The following equation is relevant to both photodiodes and photocathodes used as point detectors:

$$(S/N)_V = \frac{Me\eta [\lambda/(hc)] \sqrt{R_L} P_s}{\sqrt{4kTB + [(M^{2+x})i_D + i_L] 2eR_L B}} \quad (4)$$

where $(S/N)_V$ = voltage signal-to-noise ratio

η = quantum efficiency

M = multiplication (detector current gain)

e = electron charge

B = bandwidth = $(R_L C)^{-1} = 1/2\Delta\tau$

R_L = load resistance

x = excess multiplication noise coefficient
(an approximation)

P_s = signal power

i_L = unmultiplied leakage current

i_D = total multiplied dark current ($\sim A_D$)

= $i'_D + \eta [\lambda/(hc)] e P_b$; $P_b \sim A_D$

i'_D = true dark current

P_b = background power incident on detector of area A_D

For short pulses with low-noise detectors the quantum nature of the return signal cannot be ignored. At least two return photons need to be detected in $\Delta\tau$ (Eq. 2). For $\lambda = 1.06\mu$ and $\Delta\tau = 10$ nsec, $P_{\min} > 3 \times 10^{-11}/\eta$ watt, which for $\eta = 0.01$ corresponds to a maximum noise equivalent power (NEP) for 10-nsec pulses of 2×10^{-13} watt $\text{Hz}^{-1/2}$ set by the quantum nature of the signal. In the signal-shot-noise limit the signal-to-noise ratio while the signal is present is given by

$$[(S/N)_V]^2 = \eta(\lambda/hc)P_s/B \quad (5)$$

which shows that in this limit quantum efficiency is extremely important. Since the noise in the signal-shot-noise-limited case cannot cause a false-alarm problem, signal-to-noise ratios need not be as large for low-duty-cycle pulse detection systems as when the noise is present at all times. Thus the two signal-to-noise ratios are not

equivalent from a detection point of view, and Eq. 4 must always be considered.

Johnson noise is represented by the first term in the denominator of Eq. 4, whereas the second term represents dark current shot noise. The preamplifier noise has been assumed to be negligible compared to Johnson noise from the load resistor. If this is not the case, a high M and η will be even more important. Noise arising from variations in the background, as opposed to photon shot noise from a constant background, has been ignored since these variations will tend to be low in frequency as compared to the high frequencies involved in a short laser pulse.

Detection sensitivity can be enhanced by using narrower laser beams only if the detector FOV can be reduced. If the detector FOV can be reduced, smaller-area detectors that have less dark current (caused by background and leakage) can be used. This, in turn, is useful only if sufficient multiplication can be used to overcome Johnson noise limitations. Large-area detectors (for target designators) may have such large dark currents that the shot noise will dominate the Johnson noise without multiplication and large current gains will therefore not be useful.

The background is important since, no matter what happens to other sources of noise, photon shot noise from the background will remain. In a background-limited situation, photocathodes and diodes will have

$$(S/N)_v = \frac{\eta^{1/2} [\lambda/(hc)] P_s}{\sqrt{2J_B A_D B M^x}} \quad (6)$$

where J_B is the effective background photon flux on the detector, $\eta \rightarrow 1$ for the highest quantum efficiency detector, and $x \rightarrow 0$ for excess-noise-free multiplication. Thus, the background sets an upper limit on possible detector improvements.

III. PHOTOCATHODES

Photoemissive detectors, if their quantum efficiency is high enough, usually enjoy a considerable advantage, especially with relatively short laser pulses. The reason for this is that considerable detector current gain g (or multiplication M) is needed to overcome Johnson noise limitations if i_D is small and R_L is kept small. The maximum value of R_L is determined by RC effects and the minimum circuit capacitance, often in the 5-pf range (Ref. 4). This capacitance may be increased for larger-area diodes; however, for small devices R_L is limited to about 2 to 4 k Ω for 10-nsec pulses. A photomultiplier is the only device which can easily provide large gains (greater than 10^4) without introducing very much excess noise ($x \rightarrow 0$). Development of the electron multiplier can proceed somewhat independently of the development of the photocathode so that a cathode which is developed to yield high quantum efficiency at a given wavelength can use an already established gain mechanism. For a photodiode, the gain structure must be developed for each new absorbing material. Large-area photoemissive surfaces can be easily developed, whereas large-area avalanche diodes (diodes with multiplication) are very difficult to fabricate. Small imperfections may cause a dead spot in a photoemissive device, whereas small imperfections will cause a short in an avalanche diode which will ruin the whole device. Large-area semi-transparent photoemissive surfaces can easily be incorporated into an imaging system. Reflection mode imaging systems are possible, but only with cost and weight penalties. Reflection mode imaging would present more difficult engineering problems. Leakage currents of a photoemissive device are typically less even without cooling. The only real disadvantage of the photocathode detector lies in its lower quantum efficiency, which is usually poor in the infrared. Aging is also a problem. Photocathodes are also subject to destructive overload due to cathode surface heating.

The standard present-day commercially available photocathodes for the various interesting wavelengths have the following characteristics (Ref. 2):

	<u>Wave-length, microns</u>	<u>Type</u>	<u>η, percent</u>	<u>True Dark Current Density at 20°C, amp/cm²</u>	<u>True Dark Current Density at -20°C, amp/cm²</u>
Doubled YAG	0.53	S20	10	2×10^{-16}	
Ruby	0.694	S25	4	10^{-15}	
GaAs (cooled)	0.86	S25	0.9		
Nd ³⁺	1.06	S1	0.035	$\sim 10^{-12}$	3×10^{-15}

A maximum electron multiplier gain of 10^5 and a 20Å filter lead to the NEP shown in Table 1 ($R_L = 5 \text{ k}\Omega$ for $f = 30 \text{ MHz}$). The quantum nature of the signal has been ignored in Table 1. However, depending upon operating conditions, limitations arising from fluctuations in the signal may well dominate the low-noise, low-quantum-efficiency systems. For a 10-nsec pulse the S1 will, in fact, be limited to $P_{\text{min}} > 10^{-7}$ watt, which corresponds to an NEP of 10^{-11} watt Hz^{-1/2} and therefore will be inferior at all times to the high-quantum-efficiency avalanche diode for use as a point detector.

Several improved trialkali (S20-type) polycrystalline film cathodes (S20RX or EOS S20VR, for example) have been recently developed and give somewhat better response ($\lambda < 1\mu$) in the laboratory, i.e., $\eta = 10$ percent at 0.69μ and 3 percent at 0.86μ . Since electrons going away from the surface are generally lost, the maximum quantum efficiency which could ever reasonably be expected at these wavelengths with a photocathode is 50 percent (100 percent is theoretically possible, however, with a diffusion process). Therefore, there is not a lot of room for improvement. Nevertheless, other types of cathodes working on a new principle are available.

Quantum efficiencies of 20 percent at 0.694μ and 10 percent at 0.86μ have been obtained in reflection with Cs₂O coating on cleaved single-crystal GaAs with surprisingly low dark current densities (lower than the S20)(Ref. 5). Reflection mode GaAs photocathodes are becoming available commercially. "Quantum" photocathodes have $\eta = 0.05$ at 0.694μ and $\eta = 0.02$ at 8.6μ .

TABLE 1. DETECTOR NOISE EQUIVALENT POWER

[f = 30 MHz ($R_L = 5 \text{ k}\Omega$), Maximum Electron Multiplier Gain = 10^5 , 20Å Filter]

Detector Type	Wavelength, microns	Noise Equivalent Power, watt Hz ^{-1/2}		
		Detector Area 600μx600μ		Detector Area 250μx250μ
		Sunlit Background*	Night-time	
S25	0.694	10 ⁻¹²	10 ⁻¹⁵	
Silicon avalanche diode	0.694	3x10 ⁻¹³	10 ⁻¹³	
S1	1.06	6x10 ⁻¹²	10 ⁻¹³ (T = 300°K) 6x10 ⁻¹⁴ (T = 260°K)	
Germanium avalanche diode (T = 260°K)	1.06			10 ⁻¹²
Hypothetical photocathode ($\eta = 0.01$, $J_d = 10^{-13}$ amp/cm ²)	1.06	10 ⁻¹²	2x10 ⁻¹⁵	
Hypothetical III-V avalanche diode ($M_{max} = 200$, $x = 0.1$, $\eta = 0.7$, $J_d = 10^{-4}$ amp/cm ² , T = 260°K)	1.65			2x10 ⁻¹³ 2x10 ⁻¹² (M = 1, no surface leakage)

*FOV = 5×10^{-3} radian, f-number = 2, D = 6 cm.

Unfortunately, performance as good as this is not expected in transmission (for imaging systems) since the thin single-crystal film of GaAs has to be epitaxially grown on GaP or some other transparent

substrate and the crystalline match may cause problems. In accordance with these expectations, results in transmission have not been as good (Ref. 6). It may be necessary to resort to a polycrystalline film, but then the quantum efficiency could not be expected to be as high. There have been some suggestions that a thin enough single-crystal film could possibly be formed by etching down a bulk crystal. This would allow for good material control but the thinning problems will be severe. As most of the military interest at 0.694μ and 0.86μ involves imaging systems, and as semitransparent photocathodes are easier to incorporate into imaging systems, the greatest utility of these new types of photocathodes will involve developments at 1.06μ . The S1 is the best photocathode that is currently available for incorporation into 1.06μ laser systems, and at 1.06μ there is much room for improvement.

The quantum efficiency at 1.06μ in the S1, which has been worked on for 30 years, is still rather poor (a factor of 10^3 below the maximum expected $\eta = 0.5$) and, unless it is cooled, the dark current is high. However, it is only useful to reduce the dark current to values less than that caused by the background. For a diffuse reflector in sunlight with a 20\AA filter at 1.06μ and $f:2$ optics, the background produces a "dark" current of about $\eta 6 \times 10^{-6}$ amp/cm² so that the S1 will have about 2×10^{-9} amp/cm² with such a background and will therefore be background limited with sufficient photomultiplier gains ($> 10^4$). Operation at night will, of course, make the true dark current more important. For daytime operation, improvements can only come with increased quantum efficiency since the noise equivalent power is $\sim 1/\eta^{1/2}$ for a background-limited situation. Decreased true dark current will only be marginally useful in high-speed small detectors since gains are presently limited to 10^5 and Johnson noise effects will dominate for detector areas less than 36×10^{-4} cm², but for larger detectors the decreased dark noise produced by cooling could be useful. The point is that Johnson noise dominates if

$$i_D < \frac{4kT}{(M_{\max})^2 2eR_L} \quad (7)$$

Thus, dark current densities of $1/3 \times 10^{-12}$ amp/cm² are small enough for $M_{\max} = 10^5$, $T = 300^\circ\text{K}$, $R_L = 3 \text{ k}\Omega$, and detector diameters of 600μ . Increased quantum efficiency would help as η to the first power at night even for small-area detectors.

The proper figure of merit for a photocathode used in an imaging system depends on the operating conditions and on the properties of the intensifier used with the primary photocathode. The performance of imaging systems is ultimately determined by the shot noise of the photocathode current and the contrast reproduction of the system. If the scene is bright enough $J_s > J_d$ (J_s needs to be typically 10^{-13} amp/cm² to resolve a tank at 1000 m). The proper figure of merit is then independent of dark current and is at best proportional to $\eta^{1/2}$ (this may be degraded by the modulation transfer function; see Section X). If on the other hand $J_d > J_s$, the signal-to-noise ratio goes as $\eta/\sqrt{J_d}$. Direct view devices need to be concerned with contrast which will be proportional to η/J_d under conditions of $J_d > J_s$.

Decreased dark current down to about 10^{-13} amp/cm² is thus a useful objective. Decreased dark current can be obtained by cooling but this is not always an easy engineering or logistics problem. Increased laser power and quantum efficiency (for a given range) will increase the signal current and therefore tend to make the dark current less important. For any given performance level there is a direct tradeoff between quantum efficiency and laser power unless the detector is background limited. Thus for all active night vision systems quantum efficiency can be considered to be the primary figure of merit.

Obtaining increased quantum efficiency at 1.06μ and farther into the infrared for photocathodes is therefore of paramount interest. The dark currents (10^{-12} amp/cm² at 300°K) are good enough for small surfaces, but reduced dark current would be useful for large-area detectors.

The process of photoemission depends upon enough electrons receiving sufficient energy from the incident photons to escape from the surface of the photocathode material. A low reflection coefficient, strong absorption near the surface, and low electron scattering so that

the electrons can escape have made semiconductors the preferred photocathode material for high quantum efficiency. The S1 depends on electron emission from a metallic silver powder so that its quantum efficiency is understandably low, although it does have longer wavelength response. Unfortunately, the sum of the energy gap and the electron affinity ($E_g + E_A$ = the energy from the valence band to the vacuum level) of most semiconductors tends to be in the 4- to 5-ev range (none have been found with less than 2.0 ev) due to the usual electrostatic interactions; thus no emission will result from infrared light unless special surface treatments are used to reduce the barrier to electron emission ($1.06\mu \leftrightarrow 1.17$ ev). Much of the history of photocathode improvement in the infrared over the last 40 years has been involved with learning to apply better surface treatments, often with very little understanding as to why the new treatment brought improvements. Table 2 shows some of the properties of different types of photocathode surfaces.

TABLE 2. PHOTOCATHODE CHARACTERISTICS*

Type	Example	Reflectivity	Absorption	Electron Escape Depth	Drift Region	Surface Barrier that Limits Long Wavelength
Powdered metal with CS_2O	S1	Low (~ 50%) (powder only)	High ($> 10^4$ cm^{-1})	~ 500Å in IR	?	Possibly $E_A + \delta$ of surface material
Semiconductor	Cs_3Sb	Low (~ 40%)	High ($> 10^5$ cm^{-1} , $hc/\lambda > E_g$; high ($\sim 10^4$ cm^{-1}) at band edge if direct allowed transition, otherwise $\sim 10^2$ cm^{-1})	Deep (~ 200Å) if $hc/\lambda \gg E_g$; deeper if $hc/\lambda \sim E_g$, deeper especially if high mobility ~ 1μ	None	$E_A + E_g \sim 2-5$ ev
Cs-coated semiconductor	GaAs with Cs	Low			Band bending region; smaller if heavily p-type surface layer (70Å)	ϕ of Cs ~ 1.4 ev
Heterojunction semiconductor	GaAs with CS_2O	Low			Heterojunction spike + band bending region + surface layer	$E_A + \delta$ of surface material ~ 0.6-0.8 ev or heterojunction spike

*Desired characteristics for high quantum efficiency (maximum expected = 0.5):

- Low reflectivity
- High absorption
- Long electron scattering length
- Small drift region

Within the last four years, research on semiconductor surfaces has led to an improved understanding of semiconductor photocathodes. A heterojunction model has come to be accepted for a p-type semiconductor coated with Cs_2O even though it has yet to be proved in detail (Refs. 7, 8). This type of cathode is thought to be the only one capable of producing a high-quantum-efficiency photocathode for $\lambda > 0.9\mu$ (emission from a surface coated with Cs alone is restricted by the work function of absorbed elemental Cs). The heterojunction model does indeed give a prescription for obtaining a high quantum efficiency. A quantum efficiency of 0.2 at 0.69μ has been obtained in the laboratory with a GaAs substrate coated with Cs_2O (Ref. 5). What is preferred is a direct bandgap semiconductor with an allowed transition at the right energy $E_g = hc/\lambda$ which can strongly absorb the radiation (so that the excited electron will be close to the surface). This material should be strongly p-type (for a short band bending distance) and have high mobility and a long recombination time (for a long diffusion length). The material should be coated with a thin layer of strongly n-type material of low electron affinity (Fig. 1).

To obtain a high quantum efficiency, the electrons excited to the conduction band must be able to diffuse across the surface layer without losing too much energy and exit from the material. Poorly understood tradeoffs exist between the desire for a long diffusion length (high mobility, etc.) and the desire for strongly p-type material and between the desire for a thin surface layer and the desire for a fermi level close to the conduction band in the surface material.

It is well established, however, that to obtain high quantum efficiency at a particular wavelength, the energy gap of the principal p-type material should be just below the photon energy ($E_g = hc/\lambda - \Delta$) (Δ may be necessary due to the heterojunction spike; the influence of this potential spike is poorly understood; it may limit long-wavelength response). From photoemission measurements this barrier height for cesium oxide on gallium antimonide has been estimated to be as much as 1.23 eV relative to the bulk fermi level of the gallium antimonide (Ref. 9). Thus, for photoemitters in the 1 to 2.1μ region, the III-V

semiconductor alloys which can vary their direct energy gap with composition in the 0.5- to 1.2-ev range are the most promising photocathode material. $\text{InAs}_{1-x}\text{P}_x$, $\text{In}_{1-x}\text{Ga}_x\text{As}$, and $\text{GaAs}_{1-x}\text{Sb}_x$ (for this one $E_g > 0.7$ ev) and possibly $\text{Al}_{1-x}\text{Ga}_x\text{Sb}$ and $\text{In}_{1-x}\text{Al}_x\text{As}$ are very important (Ref. 10). III-V semiconductor alloys with larger energy gaps (corresponding to visible wavelengths) have been extensively studied for commercial application, but much less is known about those relevant to the military applications discussed here.

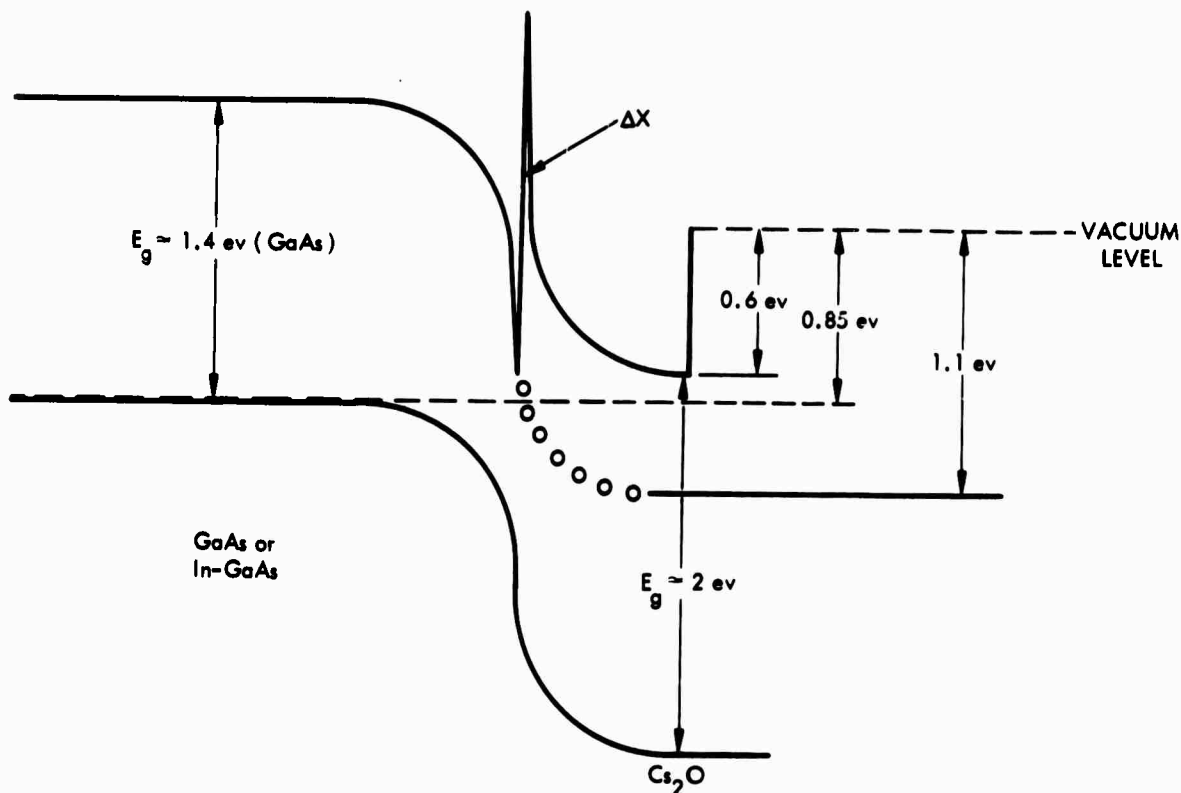


FIGURE 1. Heterojunction Energy-Level Diagram for GaAs- Cs_2O . ΔX is the difference in electron affinities of the two materials.

Calculations based upon empirical relationships derived from experiments with GaAs predict that an E_g of 1.14 ev would be optimum for 1.06μ light. These calculations predict that if a doping level of $2 \times 10^{19}/\text{cm}^3$ is used to pin E_f to the valence band edge then a transverse

electron diffusion length greater than 0.25μ should give quantum efficiencies greater than 1 percent with a Cs_2O surface. A material with a recombination time of 1 nsec needs mobilities (μ_n) greater than $25\text{ cm}^2/\text{vsec}$ to give 0.25μ diffusion lengths. Majority carrier mobilities of 70 to $80\text{ cm}^2/\text{vsec}$ are routinely achieved with p-type GaAs ($2 \times 10^{19}/\text{cm}^3$ doping level) and mobilities in the 30 to $50\text{ cm}^2/\text{vsec}$ range along the surfaces have been achieved with mixed crystals (Ref. 11).

Already very encouraging results have been obtained with Cs_2O coating on $\text{In}_{1-x}\text{Ga}_x\text{As}$ and especially $\text{InAs}_{1-x}\text{P}_x$. Quantum efficiencies greater than 1/2 percent have been obtained on a laboratory basis (not a sealed-off tube) in a reflection mode using thick (5μ), epitaxially grown (on GaAs), single-crystal thin film of 1-cm^2 area ($E_g = 1.05\text{ ev}$, $\Delta = 0.1\text{ ev}$) (Ref. 12). A quantum efficiency of 0.008 has recently been reported in reflection at $\lambda = 1.06\mu$ with $\text{InAsP-Cs}_2\text{O}$ (Ref. 12a). As far as the III-V film is concerned, what is now needed is thinner ($t < 1\mu$) film of good transverse electrical properties to make a transmission device (necessary for imaging systems). Some transmission work has been done with $\text{GaAs}_{1-x}\text{Sb}_x$ but η was low (~ 0.01 percent) (Ref. 5). Photocathode life is expected to be a critical problem.

The three mixed crystals mentioned in the preceding paragraph can be epitaxially grown from the liquid or vapor phase on convenient crystalline substrates which are transparent to radiation of 1.06μ . For 1.06μ operation, all three are at least 80 percent GaAs or InP so that these two materials can be used as substrates for transmission devices for imaging systems. A good crystalline match (expansion coefficient, etc.) is needed since, for operation with the light incident from the substrate, a thickness greater than 1μ cannot be tolerated, and the transverse minority carrier (electron) mobility must be large and the recombination time long to allow the electrons to diffuse to the exposed surface. The indexes of refraction should also match since the 1μ diffusion length is fortuitously very close to the 1.06μ wavelength of light and interference effects might otherwise ruin the uniformity of response if variations in thickness occurred (Ref. 12).

A reasonable extrapolation of the data at various wavelengths would suggest that, using Cs_2O surfaces, quantum efficiencies of 1 percent should be obtainable at 1.06μ in point detectors in field use within a two-year time frame if this work is properly supported. Claims of $\eta \rightarrow 10$ percent at 1.06μ are overoptimistic. Incorporation of these new photocathodes into a useful sealed-off tube on a production basis calls for new techniques, as vacuums of 10^{-9} torr will be necessary. Thermionic emission (not yet firmly determined) is expected to be up to a factor of 10 less than for the S1. Although some preliminary results have been discouraging, i.e., $J_d = 2 \times 10^{-10}$ amp/cm², $T = 300^\circ\text{K}$ (Ref. 13), other results with similar heterojunction photocathodes have been more encouraging, i.e., $J_d \approx 2 \times 10^{-11}$ amp/cm² (Ref. 14). It should be noted that dark currents for these cathodes are many orders of magnitude less than would be predicted by using $A = 120$ amp/cm² in Richardson's equation, using the work function of the Cs_2O surface material. The thermionic emission may well be controlled by the interface barrier between the III-V compound and the Cs_2O . A barrier of 1.17 eV would give $J_d = 3 \times 10^{-13}$ amp/cm² with $A = 120$ amp/cm² ($^\circ\text{K}$)².

A 1 percent quantum efficiency is a factor of 30 better than for the S1 so that the improvement at 1.06μ is substantial (Ref. 14).

Even if the quantum efficiency at 0.69μ increased to 20 percent, this would mean that small detectors at 1.06μ would be worse by only a factor of 3 to 10 instead of the factor of 10 to 100 which holds at present.

The possibility of extending the heterojunction cathode to the 1.5μ region exists, but the outcome is in considerable doubt. Since the energy gap of the III-V alloys can easily be sufficiently decreased, the outcome will be limited by the electron affinity of the n-type surface layer, thought to be 0.6 eV ($\lambda = 2\mu$) in Cs_2O . However, for films thin enough, the fermi level is not at the bottom of the conduction band, so that the work function tends to be 0.85 eV ($\lambda_{\text{max}} = 1.46\mu$). Some extra energy may be necessary to get through the band bending region and the surface layer--perhaps 0.05 eV per 50\AA . Thus ~ 0.15 -eV

extra energy is probably required. This would make $\lambda_{\max} = 1.24\mu$ for a Cs_2O surface. Indeed, quantum efficiencies as poor as 10^{-5} have been observed for $\lambda = 1.2\mu$ with a bandgap of 0.92 eV (Ref. 14). There is also the possibility that the heterojunction potential spike will limit the long-wavelength response since this potential barrier at the interface is expected to become larger for a greater mismatch in electron affinities (Ref. 15).

Improvements, especially at $\lambda > 1.06\mu$, might come from using other surface layers. The search for a low-electron-affinity, highly n-type material is very important. CsF might be tried. The electron affinity of Cs_3Sb is reputed to be 0.45 eV (versus 0.6 eV for Cs_2O) (Ref. 8). However, it is not known whether this material can be deposited in an n-type layer. Some experiments carried out by the Japanese that showed improved quantum efficiency upon the addition of Sb to GaAs-Cs may have demonstrated that this is possible (Ref. 16).

An alternative approach to the development of photocathodes with increased infrared response is offered by field-assisted photoemission. Field-assisted or field-enhanced photoemission, as the name implies, is an attempt to obtain an increase in the photoemissive yield or alternatively the threshold wavelength of a material through the application of an electric field. The effect of the electric field can generally be viewed as adding energy to a photoelectron excited to an initial energy state normally insufficient to surmount the surface barrier. Energy can be gained by the carrier by acceleration in some high field region, by an effective lowering of the barrier itself, or by a combination of these effects. Field-assisted photoemission is particularly attractive when it may be the only possibility. In principle, the photothreshold of a field-assisted photoemitter is limited only by the bandgap of the bulk material. Materials with high absorption coefficients and narrow bandgaps are available; however, the practical considerations involved in the production of high field conditions may have a considerable influence on the feasibility of a given device.

Several attempts have been made in the past to obtain field-assisted photoemission from reverse-biased Schottky diodes (Ref. 17), and p-n junctions (Refs. 18 to 21), but have failed to produce quantum efficiencies above 10^{-4} although field assistance did yield infrared response.

In the ideal case for a reversed-biased Schottky diode made with aluminum on silicon, minority carriers are generated in the p-type silicon by the incident radiation and diffuse to the depletion region where they are accelerated by the applied field, entering the aluminum as hot electrons. Those electrons retaining sufficient energy in the direction normal to the surface are ejected into the vacuum. Photo-response measurements have been made by Miyaji and Hasegawa (Ref. 17) on a sample with a bulk carrier density of about $1 \times 10^{16}/\text{cm}^3$. At zero bias they obtained the usual response for a cesiated metal surface indicating a work function of 1.6 eV for the cesiated aluminum. At 10.5 volts bias they obtained the additional field-assisted component out to about the silicon band edge. The quantum efficiency over the fairly flat portion of this component is about 5×10^{-6} .

The energy loss mechanisms considered in an analysis of these data by Miyaji and Hasegawa (Ref. 17) were the transmission of the light through the 100\AA aluminum film, electron-hole recombination during diffusion to the depletion region, phonon emission in the depletion layer, and attenuation in the aluminum. Losses due to pair production in the depletion layer were not included since the field strengths involved were near or below the threshold values.

A qualitative understanding of the results was possible, although the predicted and experimental transfer curves differed by orders of magnitude, probably due to the silicon-aluminum interface. The calculations suggested the use of a lower resistivity material. However, heating due to dark current can appreciably affect the photocurrent both by raising the lattice temperature and by causing physical deterioration of the junction. Recent data for samples with bulk carrier densities of 3 to $4 \times 10^{16}/\text{cm}^3$ confirm the theoretical predictions in that the quantum efficiency of the field-assisted component is an order

of magnitude higher than in previous samples. In addition, work has been initiated on p-type germanium-aluminum contacts in order to obtain sensitivity farther into the infrared.

The reverse-biased p-n junction photoemitter consists of a p-type semiconductor overlaid with a thin n-type layer whose surface work function has been reduced by cesium treatment. The photoexcitation occurs in the p-type region of the junction. Photoelectrons diffuse to the junction where they are accelerated by the field through the reverse-biased depletion region to an energy sufficient to surmount the reduced vacuum barrier.

Measurement of the quantum efficiency of silicon p-n junctions were made by Simon and Spicer (Ref. 18). They found a significant increase in the emitted photocurrent out to the silicon band edge due to the field-assisted component. For this work, the junctions intercepted the surface across the face of the sample bar. Later work was performed to fabricate junctions parallel to the surface by heat treatment or diffusion in order to obtain larger emitting areas. Although the results for quantum efficiency were no better, there were qualitative indications that thin n regions could be formed and resulted in field-assisted photocurrents. However, heat treatment yielded surfaces whose work function could not be reduced below about 2 ev even with cesium treatment while very thin diffused junctions tend to be nonuniform.

Simon and Spicer (Ref. 20) at RCA and later Davies and Thornton (Ref. 21) at the University College of North Wales in Great Britain have measured field-assisted photoemission from germanium p-n junctions. The results of both of these studies showed a field-assisted component out to the germanium band edge but differed in detail for both the zero bias and the applied bias curve.

The fundamental energy loss mechanisms in this approach are due to optical phonon emission and pair production in the depletion layer and n-type region of the semiconductor. An analysis of the field-assisted photoemission data for silicon was performed by Simon and Spicer (Ref. 18) who collected the loss factors at a fixed bias into a transmission

coefficient. It was possible to fit the data with a transmission coefficient of 7×10^{-5} and a diffusion length of 2×10^{-3} cm.

While infrared response to wavelengths corresponding to the band-gap energy of the p-type semiconductor is observed in the reverse-biased junction emitters, the quantum efficiency is low in the field-assisted region. In general, low efficiency results from the difficulty of fabricating the junction close enough to the surface to reduce the thickness of the layer which must be traversed by excited electrons.

The most promising approach to field-assisted photoemission is based on electron tunneling. It offers the possibility of avoiding the necessity of meeting conflicting requirements in the same material for the heterojunction and the low photoelectron escape probability associated with hot electron emission encountered in the reverse-biased junction emitters. The tunnel emitter combines photoexcitation in a small bandgap semiconductor with emission from a negative affinity (surface treated) wide bandgap semiconductor. In principle, this approach could be applied to the development of photocathodes with photoelectric threshold in the intermediate infrared for image-sensing thermal radiation.

The energy level diagram of this photon induced tunnel emitter is shown in Fig. 2. The structure consists of a p-type infrared sensitive semiconductor such as germanium or silicon covered with a thin insulating layer. The insulator in turn is overcoated with a second p-type semiconductor such as gallium phosphide which shows the negative electron affinity effect at the interface with vacuum. For the purpose of this discussion, silicon and gallium phosphide will be used as the semiconductors.

Bias is applied to the structure as a positive voltage to the gallium phosphide and a negative voltage to the silicon. If the resistivities of the semiconductors are sufficiently low, most of the field appears across the insulator. Photoelectrons are generated as minority carriers in the silicon whereupon they diffuse to the silicon-insulator interface. These photoelectrons then tunnel into the

insulator conduction band from which they drift into the gallium phosphide under the action of the applied field. Due to the negative electron affinity effect of the gallium phosphide, these carriers now have a high probability for emission into vacuum once they have diffused to the surface of the gallium phosphide.

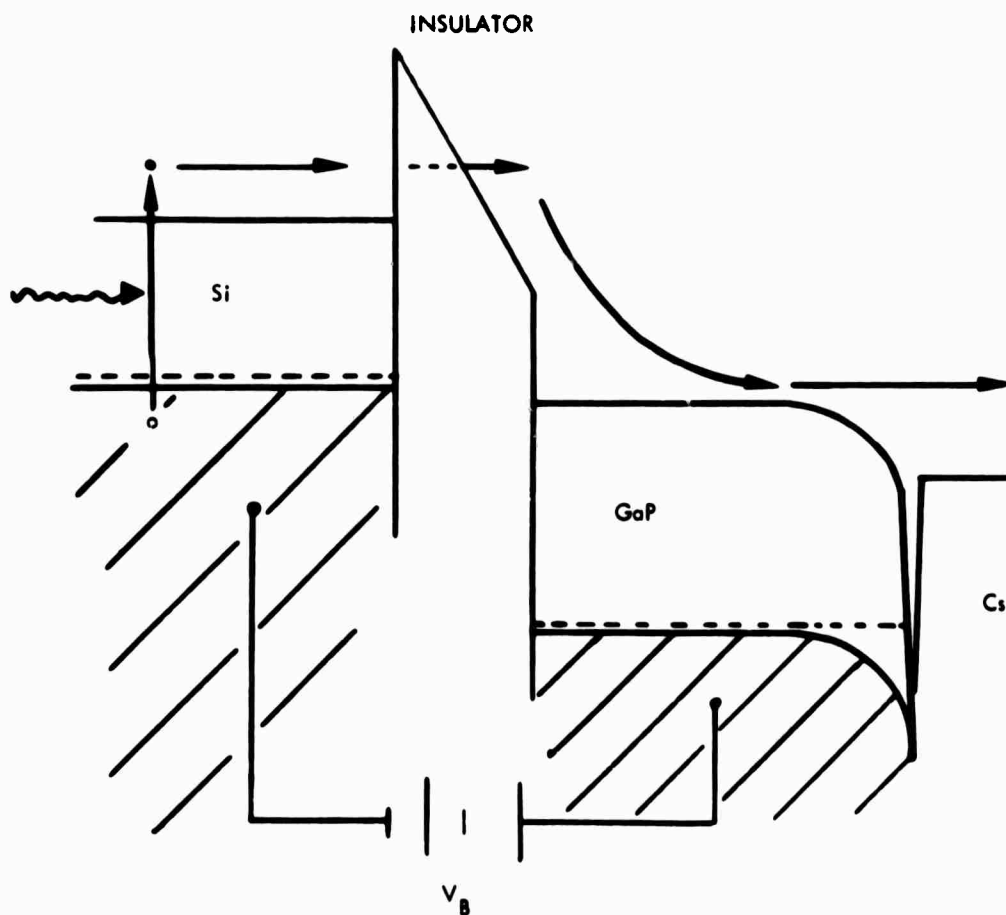


FIGURE 2. Photon Induced Tunnel Emitter.

This configuration, in principle, is not adversely affected by the fundamental mechanisms which limit the quantum efficiencies of conventional photoemitters and other field-assisted approaches. These loss mechanisms include the loss of photoelectron energy by phonon emission, pair production, and hot electron attenuation in metals and surface layers and attenuation of photoelectron currents by high surface barriers. Since the photoelectrons injected into the treated

gallium phosphide encounter virtually no surface barrier, it is possible for these carriers to escape after having been completely thermalized in both the insulator and gallium phosphide conduction bands. On the other hand, in addition to the materials problems of photon absorption in the detecting semiconductor, the minority carrier lifetimes in both semiconductors, and the reliable production of negative electron affinity surfaces, there is the question of the injection efficiency for the transfer of photoelectrons through the insulator. This injection efficiency is determined by the details of the interface step between the conduction bands of the photodetecting semiconductor and the insulator and the field distribution within the insulator. In the ideal case, the biased insulator is represented by a trapezoidal barrier with an assumed infinite bandgap.

The majority of the experimental work (Ref. 22, 23) to date has been concentrated on the photoelectron tunneling process in metal-insulator-semiconductor or MIS diodes. Research on the negative electron affinity effect in III-V semiconductors has been performed concurrently but few results are as yet available on the combined device. RCA has observed a quantum efficiency in one device of approximately 0.5 percent at 1.06μ . Quantum efficiencies in the MIS diodes themselves of 10 to 20 percent are common without correction for light transmission through the gold electrode.

The tunnel photocathode is a long-range approach to an infrared photocathode. It offers high potential payoff, but difficult materials problems must be solved and the risk is correspondingly high.

New surfaces and biased field devices are important for eye-safe wavelengths, but they are far less certain than improvements at 1.06μ using Cs_2O , which on a laboratory basis have already been demonstrated in reflection at least. Photocathodes for $\lambda > 1.5\mu$ will not come quickly.

The use of these new surfaces in electron multiplier tubes may make gains greater than 10^5 practical. Such gains, combined with the higher quantum efficiencies, could make 2- to 5-nsec pulses attractive

where laser materials damage problems did not come in (Ref. 24). High quantum efficiencies with these new diffusion-type photocathodes may result in long escape paths and thus cause a dispersion in electron escape times that will ultimately limit the frequency response of these detectors. As an example, for $T = 300^\circ\text{K}$ and $\mu_n = 1000 \text{ cm}^2/\text{vsec}$ the escape time for a 2μ path is 1.5 nsec. The use of a configuration that required much longer escape paths could seriously degrade the frequency response of the photocathode since the escape time is proportional to the square of the escape distance. Near an absorption edge the effective quantum efficiency tends to be both wavelength and frequency dependent.

IV. AVALANCHE DIODES

Probably the only way to get really high quantum efficiency (approaching 1) with radiation $\lambda > 1\mu$ is to use an internal photoeffect device such as a photodiode. For short pulses, high gains are still useful; thus avalanche photodiodes are used where some multiplication takes place in the depletion region. Current gains greater than a few hundred are hard to achieve (local breakdown occurs). Leakage current and the "true" dark current are high. The multiplication is often not even approximately noise free [$x \sim 0.4$ for Si and 1 for Ge (Eq. 4)] so that the optimum value of M is less than one would predict for a device free of multiplication noise and depends on the size of the dark current (Refs. 25, 26).

An elaborate voltage stabilization circuit is necessary to control the multiplication. An excellent technology is required to make avalanche devices with low enough leakage currents free of local breakdowns. Even with such well-known materials as silicon and germanium, yields are such that diameters larger than 1 mm are not obtained. The requirement for a well-developed technology involving good surface passivation has at this stage suggested the elemental semiconductors, i.e., Ge and Si. Unfortunately, their absorption edges are really not at the proper wavelength for the lasers of interest. Any diode detector must absorb the radiation in the high field depletion region to resolve a short pulse. Thick depletion layers require high-resistivity

substrate material and the yield tends to decrease with the volume of the depletion region. Thus, depletion widths are presently limited to 50μ in Si and about 20μ ($3\ \Omega\text{-cm}$ material) in Ge (Refs. 27, 28). Since the half-power absorption depth at 1.06μ in Si is $\sim 500\mu$, the quantum efficiency is < 1 percent for 30-nsec pulses, so that silicon avalanche diodes are not used for Q-switched pulses at 1.06μ although they would do very well with pulses longer than $10\ \mu\text{sec}$. Unless absorption can occur in a region of large electric field (as in a PIN diode), Si is an inappropriate detection material for 1.06μ laser systems. Si avalanche diodes are, of course, perfectly appropriate for GaAs injection laser systems. Germanium avalanche diodes can give quantum efficiencies of 0.6 at 1.06μ and 1.54μ ; however, they will encounter quantum efficiency problems with short pulses for $\lambda > 1.6\mu$, as the absorption has been reduced to $\sim 100\ \text{cm}^{-1}$ by 1.6μ at 300°K (Ref. 29). The absorption at 1.6μ is even less with cooled devices, although the Franz Keldish effect may help (Ref. 30). The exact cutoff for 30-nsec pulses has yet to be determined. In that length of time, at 300°K the electrons could be expected to diffuse only about 15μ , so that an absorption coefficient greater than $500\ \text{cm}^{-1}$ is needed.

Unfortunately, germanium is in principle a poor avalanche diode material. The ionization coefficients for holes and electrons are rarely more than a factor of 2 apart, which leads to large excess multiplication noise ($x \sim 1$). One would like to make p on n junctions; however, it has proven impossible to make such diodes so that n on p is accepted, but then the x is even a little greater than 1 (Ref. 27).

The dark current which is eventually multiplied in germanium diodes for 1.54μ is $3 \times 10^{-2}\ \text{amp/cm}^2$ at 300°K (versus $3 \times 10^{-7}\ \text{amp/cm}^2$ for Si), which is so high (sunlit background $\sim 10^{-6}\ \text{amp/cm}^2$) that in practice the detector is operated cooled with $3 \times 10^{-3}\ \text{amp/cm}^2$ at 260°K (Ref. 27). Leakage currents for detectors of 10-mil diameter are $\sim 3\ \mu\text{amp}$ at room temperature. An M of 100 can be obtained, but the noise properties are such that M over 10 is detrimental at 300°K and M over 25 is detrimental at 260°K . A thermoelectric cooler which draws $1\text{-}1/4$ watts is used to hold 260°K (Ref. 27). Antireflection coatings have been successfully applied (Ref. 28). An NEP of $10^{-12}\ \text{watt Hz}^{-1/2}$ is

available at 30 MHz at 260°K in a 10-mil device at 1.06 μ (Ref. 27). Larger-area devices will not do as well ($NEP \sim A_D^{1/2}$).

Germanium diodes for 1.06 μ use stronger p-type doping and have thinner depletion regions; the diffusion and space-charge-generated dark current density can, therefore, be less than 5×10^{-3} amp/cm² at room temperature (Ref. 26). The only possibility for extending the high-speed response of Ge and Si to marginally longer wavelengths involves using Schottky barrier avalanche diodes which could possibly use more intrinsic substrates for a thicker depletion region.

V. AVALANCHE IN III-V COMPOUNDS

The possibility of fabricating avalanche diodes from III-V semiconductor compounds (such as InAs) and eventually from III-V alloys (much more difficult) is an interesting alternative. The main attraction of these materials involves the hope for multiplication free of excess noise ($x \rightarrow 0$) since the ionization coefficients for holes and electrons are far apart (only electrons multiply). A multiplication of 100 practically free of excess noise ($x = 0.1$) has been observed in GaAs (E_g too large) (Ref. 31). In InAs, multiplication of 10 to 15 has been observed (Ref. 32). Here the energy gap is so small ($\lambda < 3\mu$ can be absorbed) that temperatures of 77°K are necessary to reduce the dark current. These results have been obtained only on a laboratory basis and the technology development will be difficult, especially for those potentially more useful III-V alloys and compounds with E_g in the 0.5- to 1.1-ev range.

Ion implantation techniques, which have proved their worth in increasing the lateral uniformity and yield of "larger" area Si avalanche devices, may help circumvent some of the difficulties of fabricating the guard ring structure (Ref. 33). The guard ring is necessary to prevent premature breakdown at the surface and is difficult to make by diffusion processes unless excellent surface passivation is obtainable. If really large multiplication can be used, surface leakage is less important.

An ideal avalanche diode ($M_{\max} = 300$, $x = 0.1$, $J_d = 10^{-4}$ amp/cm²) would have an NEP of 2×10^{-13} watt Hz^{-1/2} for a 10-mil diameter at 1.65 μ with $R_L = 5$ k Ω ($f = 30$ MHz).

VI. LARGE-AREA DIODES

Laser target designators need large-area quadrants (FOV ~ 0.5 radian) which requires an individual detector of ~ 1 cm² area. Under sunlit conditions, the background is now appreciable [$J = \eta 3 \times 10^{-4}$ amp/cm², $\lambda = 1.06\mu$, 200 \AA filter (necessary for the large FOV), $D = 2$ cm]. If the quantum efficiency is near unity and R_L can be more than 1 k Ω ($C < 20$ pf, $\Delta\tau = 10$ nsec), the Johnson noise will be comparable to the background noise so that gains greater than one will not be needed to achieve the background-limited operation of $\text{NEP} = 4 \times 10^{-9} / \sqrt{\eta}$ watts. If the dark current densities are less than 10^{-5} amp/cm², higher-sensitivity operation at lower backgrounds could be achieved if some gain were introduced. Gain greater than one would also be more useful with shorter pulses.

PIN photodiodes ($\eta \sim 0.8$) are usually used (the intrinsic part to decrease the capacitance and, with Si at 1.06 μ and Ge at $> 1.5\mu$, to increase the absorption in the depletion region). Avalanche diodes cannot be fabricated in large areas and photocathodes have a poorer background-limited response (smaller η). Quadrant photomultipliers are available and require a dissecting of the image plane (Ref. 34). Ordinary diodes do not have the dynamic range problems inherent in a high-gain device. This is of importance for detectors for target designators. Since simplicity and low cost are a prime consideration in a throwaway system (quadrant photomultipliers are relatively expensive) and backgrounds are limiting in sunlight, it is unlikely that a photomultiplier will replace the diode except possibly for night use in nonthrowaway systems.

To achieve reasonable performance, the dark current must be reduced to $\sim 10^{-5}$ amp/cm². The dark current is satisfactory in Si PIN diodes $\sim 10^{-6}$ amp/cm² (300 $^\circ$ K) for 1.06 μ , but the large-volume

germanium diodes designed to absorb 1.65μ parallel to the junction must be cooled to 195°K (large-volume depletion regions are possible if no avalanche is required) (Refs. 2, 29). Diodes made from a III-V alloy with a bandgap just slightly smaller than that of Ge could use smaller depletion regions which would lead to reduced dark currents at room temperature, thus eliminating the necessity for cooling at 1.65μ . (Increased capacitance might be a problem but a favorable compromise could be reached if the doping level of the III-V alloy could be sufficiently varied.)

Unless lithium drift compensation techniques can be developed for the III-V materials to produce the "intrinsic" part of a PIN structure, very intrinsic material is needed to avoid excess capacitance with a large-area diode. As a practical example, if the reverse bias field must be less than $10^3/\text{cm}$, an abrupt junction model will predict that material with N (donors or acceptors) less than $10^{15}/\text{cm}^3$ is needed to hold the diode capacitance to less than $400 \text{ pf}/\text{cm}^2$ ($\epsilon = 15$). This would call for a reverse bias of 20 v and a depletion region 400μ wide.

It is unfortunate that large-area quadrants are so easily background limited as increased sensitivity would allow for longer standoff ranges. As the detector is delivering nearly ideal performance, improvements can only come by further subdividing the FOV, using narrower filters specially positioned within the optics or some form of time gating in the signal processing. This processing could easily take advantage of the known laser designator repetition rate to allow for the use of a low detection threshold without introducing intolerable false-alarm rates.

In the III-V semiconductor alloys, the bandgap can be optimized for the laser wavelength and detection process of interest. Although the technology may prove difficult (for example, flaw densities less than $10^{16}/\text{cm}^3$ are hard to obtain), the possible advantages should be clear: the material can be designed for the laser wavelength and the device need not be compromised to overcome the limitations of the material at the particular laser wavelength. The requirement for an optimal bandgap for photocathodes has previously been explained. In

diodes (avalanche or not), too small a bandgap E_g leads to absorption too near the surface and more noise (dark current $\sim e^{-E_g/kT}$) at room temperature than necessary, while too large a bandgap leads to low quantum efficiency and makes large depletion regions using very intrinsic materials necessary, which also leads to excess noise (diffusion or space charge generated). The previously mentioned III-V alloys can cover the relevant range of wavelengths and, in contrast to alloys of Ge and Si, have the additional advantage of a direct bandgap.

Alloys of II-VI compounds can also be made to vary their bandgap in this region as well. $Hg_{1-x}Cd_xTe$ has been very successful as a photoconductor for longer wavelengths. The French have made successful diodes for longer wavelengths but the more difficult metallurgy of this material (especially for high x) has limited progress. Nevertheless, diodes have been fabricated for the 1.5μ to 2μ region (Ref. 35). Room temperature dark current densities are satisfactory ($\sim 10^{-4}$ amp/cm²) (Ref. 36) but the formation of junctions close enough to the surface to allow for good response to short Q-switched pulses remains a serious problem. Large diode areas will prove very difficult.

VII. PHOTOCONDUCTORS AND AC BIAS

The use of photoconductors for high-speed detectors ($f = 100$ MHz) has always been somewhat restricted. Photoconductive gains ($E\mu\tau/l$) larger than unity are hard to achieve for the required short recombination times, especially for detectors with a useful surface area. High-resistivity material has space-charge-limited current problems at high-bias fields and low-resistivity material encounters heating problems. In any case, the maximum useful photoconductive gain (intrinsic photoconductivity) is ultimately limited to the mobility ratio due to minority carrier sweepout effects. As a practical example for $\tau = 10$ nsec, $\mu = 5 \times 10^4$ cm²/vsec, $E_{max} = 50$ v/cm, $l = 100\mu$, the gain comes out to be 2.5.

The use of a microwave-bias electric field is an attempt to circumvent those limitations (sweepout and space charge injection) caused

by the presence of contacts (Ref. 37). Higher electric fields can be used and the impedance transformation of a high-Q microwave cavity can increase the apparent current gain. Heating or velocity saturation effects will limit the electric field. The use of microwave circuitry is an important inconvenience, and it turns out that serious excess noise in the microwave components, AM and FM microwave source noise, and traveling-wave tube noise limit the performance. For efficient operation, the microwave field must penetrate the sample and the losses in the sample must be kept small to keep a sufficiently high Q for the needed impedance transformation (although FM noise may be less severe with a lower Q). How Johnson noise from the detector is transformed to the external circuit is still an open question. The best performance is, therefore, obtained only with very small ($10\mu\times 25\mu\times 25\mu$ at present) samples of high resistivity $> 10\Omega\text{-cm}$. This tiny detector area is unfortunate from a system point of view even for a point detector (it limits the size of the receiving optics for a given FOV) and the small detector volume means that this technique can be used only when the material is highly absorptive; germanium probably will not work too well at 1.65μ (because of poor absorption and because 50 times the present volume of Ge would be necessary) and low-resistivity, less intrinsic materials probably will not do too well either.

Nevertheless, very small microwave circuitry has been made for this device and progress will undoubtedly follow the progress of low-noise microwave components. With the most ideal material (high-resistivity Ge at $\lambda \leq 1.5\mu$), apparent gains of several hundred have been observed at $B = 30$ MHz and $T = 300^\circ\text{K}$ with considerable excess noise which limited the NEP to 10^{-12} watts for $f = 30$ MHz (Ref. 37). This is excellent performance, but it should be remembered that the diameter (25μ) of the detector is a factor of 10 smaller than for most small avalanche diodes; $f:l$ limits the receiver optics to $D = 0.5$ cm. A telescope could be used, but this would just add to complexity. If the same complexity were allowed for avalanche devices, similar NEPs could be obtained. If a suitable material were found, this technique might, however, be useful at 1.65μ where no other gain devices are available. The ac bias technique will undoubtedly be limited for some time to single point detectors.

VIII. HETERODYNE

A heterodyne system using a local laser oscillator to mix with the return signal in a square law detector should in principle have a minimum detectable power of

$$P_{\min} = \frac{2h\nu B}{\eta} \sim 4 \times 10^{-12} \text{ watts} \quad (8)$$

for $B = 30$ MHz, $\lambda = 1.5\mu$, and $\eta \sim 0.5$ (Ref. 38). This compares with 5×10^{-9} watts for direct detection with an NEP of 10^{-12} watt Hz^{-1/2}. A heterodyne system is an energy detector (rather than a peak-power detector), so that it is really more appropriate for cw or long-pulse operation. Since the return signal and the local oscillator should be in a spatial phase coherence across the face of the detector, there are severe problems in trying to detect diffusely reflected light with a heterodyne system. Only that portion of the return beam falling within a diffraction-limited resolution element of the optics will be useful. The coherent FOV of the detector is thus $\sim \lambda/D \sim 10^{-4}$ radians for $D = 1$ cm. Thus only 1/2500 of the return from a 5-milliradian beam will add in phase. This severely limits the performance of a system which would be complex in any case. This technique may have some usefulness when diffraction limited beam divergence is possible or when the targets subtend a very small angle, but this is not the case for the applications discussed in this report.

IX. AMPLIFICATION AND UPCONVERSION

With the advent of laser amplification and investigation of nonlinear optical effects, a number of schemes have been proposed for low light level amplification and frequency upconversion. Amplification of a laser return signal can be achieved by (1) passing the signal through an active medium in which energy level population inversion is generated with a pump, and (2) using a regenerative parametric amplifier. In a parametric amplifier the dielectric indices of a crystal are electric field dependent and consequently a nonlinear

interaction is set up between the signal, the pump, and an idler frequency which can lead to a condition of gain for the signal. Both of these amplification processes are fundamentally limited by random spontaneous photon emission. The equivalent input noise-power from this source is equal to $h\nu B$ where B is the bandwidth. Thus for the very best possible laser or regenerative parametric amplifier, the signal will equal the noise if the signal consists of exactly one photon per resolution time. However, the incoming signal photons are distributed in time according to the Poisson distribution; therefore, we need an average arrival rate of approximately seven photons per resolution time in order to equal the spontaneous emission 99 percent of the time.

A particular laser preamplifier configuration (Ref. 39) which ought to approach the fundamental spontaneous emission noise limitation has been proposed recently. This involves a bundle of fiber laser preamplifiers in front of a photocathode. The preamplifier consists of a low-loss neodymium-doped glass core with a higher index of refraction than glass cladding. The core and cladding function is an optical wave guide filled with an active medium. A second glass cladding is doped with samarium to absorb 1.06μ radiation escaping through the first cladding.

The fiber may be inserted between the collecting optics and detector of a conventional optical receiver and, by optical pump excitation designed to produce a population inversion, made to function as a preamplifier. It is well known that laser amplifiers have been generally considered impractical for amplification of low-intensity radiation due to high background radiation produced by spontaneous emission. However, it is claimed that if the laser preamplifier is made to support only the optical mode of lowest order, then the noise due to fluctuations in the spontaneous emission rate will be less than the noise produced in detectors of 1.06μ radiation. Thus, it is claimed that use of the fiber laser preamplifier will improve the signal-to-noise ratio or alternatively permit detection of a smaller optical signal. However, careful analysis indicates that as a point detector the conventional uncooled S1 photomultiplier exhibits a lower minimum

detectable signal than the fiber laser preamplifier. Cooling further improves the SI by reducing the thermionic dark current but would have no effect on the spontaneous emission noise of the laser amplifier. Careful analysis also indicates that in the image-sensing application the performance of the SI image intensifier is orders of magnitude better than can be expected from an array of fiber laser preamplifiers.

An analysis of the fiber laser preamplifier performed by E. Snitzer (Ref. 39) concluded that the minimum detectable signal (MDS) is related to the signal-to-noise ratio (S/N) by

$$\text{MDS} = (2N_e \tau \text{ S/N})^{1/2} \text{ photons} \quad (9)$$

where τ is the integration time and N_e is the number of photons emitted spontaneously in a length for which the gain is e (Ref. 39). Snitzer showed that N_e is approximately 6×10^{12} and then

$$\text{MDS} = 346(\text{S/N})^{1/2} \text{ photons} \quad (10)$$

for a 50-MHz bandwidth. Experimentally a value of $140(\text{S/N})^{1/2}$ was observed for the MDS.

The minimum detectable signal of a photomultiplier is given by

$$\text{MDS} = (1/\eta F')(J_d A / 2eB)^{1/2} (\text{S/N}) \text{ photons} \quad (11)$$

where η is the quantum efficiency of the cathode, F' is the excess noise of the photomultiplier, J_d is the dark current density, A is the area of the photocathode, e is the electron charge, and B is the bandwidth of the electronic amplifier. The quantum yield of the SI photocathode at 1.06μ is 3.4×10^{-4} , F' is approximately 1.2, J_d is approximately 10^{-12} amp/cm². If we let B equal 50 MHz, then the MDS is given by

$$\text{MDS} = 600 A^{1/2} (\text{S/N}) \text{ photons} \quad (12)$$

Thus, the measured MDS of a fiber laser preamplifier is approximately equal to the MDS of an S1 photomultiplier with an uncooled 0.5-cm^2 photocathode surface. Cooling or decreasing the area of the S1 would cause its performance to surpass that of the fiber laser amplifier.

In order to compare the S1 image intensifier with an array of fiber laser preamplifiers, it is necessary to calculate the MDS of a picture element, taking into account that the integration time of the eye is approximately 0.2 sec. Thus, the MDS of a single fiber is given by

$$\text{MDS} = 1.5 \times 10^6 (S/N)^{1/2} \text{ photons} \quad (13)$$

The area of a fiber is about 10^{-5} cm^2 . Thus, the MDS of a picture element of this area on an S1 image intensifier is given by

$$\text{MDS} = 9 \times 10^3 (S/N) \quad (14)$$

The MDS of a picture element of area 10^{-5} cm^2 is smaller by a factor of approximately 167 with an S1 image intensifier than with an array of fiber laser preamplifiers. Improvements in photocathode quantum efficiency of at least a factor of 10 are expected in the immediate future with development of the indium-gallium arsenide photosurface treated with cesium oxide. Thus, the fiber laser preamplifier cannot compare in minimum detectable signal with a photomultiplier.

Frequency upconversion has been proposed as a means for converting signals at infrared frequencies where photocathode responsivity is low to higher frequencies (shorter wavelengths) where photocathode sensitivity is high and as a means for avoiding spontaneous emission noise (if detection occurs at the sum frequency). A large number of schemes have been proposed and investigated, including voltage control of a visible electroluminescent material by means of an infrared sensitive photoconductor, control of electron or hole injection into an electroluminescent semiconductor by means of an infrared sensitive photoconductor, parametric upconversion in a nonlinear crystal, and the Bloembergen infrared quantum counter.

Parametric upconversion which has received considerable attention consists in a complex system of mixing the return signal in an optically nonlinear crystal with radiation from a pump laser and then detecting at the sum frequency. Conversion quantum efficiencies of 1 percent for point upconversion have been achieved. This was done using a Q-switched ruby pump (1.9 Mw/cm^2) and 1.7μ signal radiation with a LiNbO_3 nonlinear crystal (Ref. 40). Point upconversion quantum efficiencies could easily reach 10 percent but the real interest is in imaging systems in which conversion quantum efficiencies of only $\sim 10^{-8}$ have been achieved. In the future, conversion quantum efficiencies of 10^{-4} for a 500×500 resolution image can be expected (Ref. 41).

These techniques introduce a requirement for pulsed laser transmitters so that a high-peak-power pulsed pump can be used. In a nonlinear process, the quantum efficiency will depend on the peak power of the pump (as well as on the nonlinear coefficients and crystal length). The pump can be used to gate the imaging process.

Nonlinear crystals with large nonlinear coefficients that can be properly phase matched are needed. Optical damage from pump radiation could be a problem, but it should be remembered that, in contrast with second harmonic generation, these techniques need not produce large radiation intensities in the visible. The damage threshold for IR pump radiation with LiNbO_3 would be over 100 Mw/cm^2 , well above the pump intensities used in the example of point upconversion quoted above (Ref. 42).

LiNbO_3 , however, cannot be phase matched at 1.06μ so as to use the transmitting laser on the pump (Ref. 41), so this configuration could only use KDP which has lower nonlinear coefficients. At any rate it is certain that for 1.06μ radiation, improved photocathodes will tend to make these systems uncompetitive.

If, on the other hand, it turns out that even for specialized imaging applications longer wavelength lasers are necessary, then upconversion is more attractive. At this point, upconversion with nonlinear materials should probably be looked at as one more possible application of these materials.

A Bloembergen quantum counter which uses four energy levels could serve as a narrow-band upconverter without problems of spontaneous emission (Ref. 43). However, the quantum counter material would have to match the laser emission exactly and no suitable material has been found for 1.06μ .

X. LASER IMAGING SYSTEMS

An important application of lasers in military systems is as a source of supplemental illumination to extend the performance of night vision systems. Image intensifier (II) and low-light-level television (LLLTV) systems can be used with moonlight and starlight and can make use of the airglow. However, artificial illumination is needed for:

- Viewing at extended ranges
- Viewing under very low light levels resulting from cloud cover or forest cover
- Viewing through obscuring atmospheric conditions such as smoke, fog, dust, or rain
- Viewing past bright intervening light sources
- Viewing through camouflage nets.

Searchlights with low-density red filters are currently used to enhance scene illumination. Unfortunately, the advantage of higher scene illumination provided by searchlights is partially offset, especially under adverse atmospheric conditions, by backscatter which causes a reduction in contrast and hence in visibility of targets against background. In addition, scene irradiance achievable with searchlights is limited by the minimum beam divergence of about 5 deg (searchlight $D = 1$ ft). Backscatter can be reduced in some cases by physically separating the searchlight and viewer so that the searchlight beam and line of sight are not collinear. Clearly this approach is of limited application. Narrow beam laser line-scan systems reject backscatter originating near the transmitter if the scan rate is fast enough and a narrow FOV is used. Another approach is to use a pulsed-laser, gated-viewer night vision system.

These systems consist of a pulsed laser illuminator and a gated image intensifier tube which may be the first stage of either a

three-stage image intensifier direct view system or a remote view television system. The effect of backscatter from smoke and fog on contrast is reduced by activating the gatable image intensifier only during a small interval of time which includes the returning laser pulse reflected from a zone at some selected distance from the viewer. The effect of bright intervening lights on contrast is greatly reduced both by utilizing a narrow band pass (200Å) filter centered at the laser wavelength and by virtue of time discrimination.

The choice of photocathode for the first-stage image intensifier tube will depend on the spectral response of the cathode and the wavelength of the laser as discussed in Section III of this report. Improvements in broad-band photocathode response designed to achieve better performance in passive operation with moonlight and airglow are not intended to and will not necessarily result in better performance at specific laser wavelengths. To ensure better performance at specific laser wavelengths, it is necessary to support research for this specific purpose, keeping in mind the potential payoffs. For example, for the same performance, doubling the photocathode quantum efficiency will allow a reduction in laser power to one-half, with concomitant reductions in power supply, size, weight, and cost. For the same laser power, doubling photocathode quantum efficiency will result in better system performance. However, in order to determine the effect of cathode improvements on photoelectronic imaging system performance, both active and passive, it is necessary to evaluate the overall performance as a function of all the system parameters. The performance of other parts of the system besides the primary photocathode needs to be considered. Evaluation will reveal some rather surprising but important conclusions.

It has been established that the probability that a viewer will detect an image on a phosphor display depends both on contrast and S/N. Thus, the quality of image reproduction on the display of a photoelectronic imaging system is determined not only by aberrations in the image-forming components and transducers which affect contrast, but also by the S/N of the output image formed from electron-induced scintillations on the phosphor display.

The effect of aberrations is to cause an overlapping of the radiance pattern on the display produced by the input image irradiance. In the limit of small image element sizes, as contrast between adjacent image elements falls below a few percent, visual performance approaches zero. It has become customary to evaluate the effect of aberrations on contrast by considering the reproduction of the modulation amplitude of a sinusoidal, spatially modulated radiant test pattern as a function of spatial frequency. In principle, any radiant input image can be decomposed into its two-dimensional frequency spectra by the Fourier transformation. The principal spatial frequencies of the radiant image of a target with linear dimension L extend from zero to the reciprocal of $2L$. The ratio of the modulation amplitude of the display image to the modulation amplitude of the input image on the photocathode as a function of spatial frequency is the modulation transfer function.

In order to make a quantitative evaluation of the effect of system parameters on the overall performance of photoelectronic imaging systems a specific example is illustrated in Fig. 3. This figure shows the resultant modulation on the display as a function of spatial frequency of a typical triple intensifier with 0.30 input modulation at all frequencies. Several curves of modulation amplitude required on the display by the eye for 50 percent detection probability in unlimited time as a function of spatial frequency are also included, assuming that an S/N of 2 would be required. Each required modulation amplitude curve corresponds to a different illumination level and quantum efficiency. These curves result from an application of the fluctuation theory of visual perception of electronic scintillation images by Rose (Ref. 44), Coltman (Ref. 45), and Coltman and Anderson (Ref. 46). A requirement for an S/N of 2 corresponds to the result obtained by Schade (Ref. 47) for 50 percent detection probability in unlimited viewing time with a standard Air Force 3-bar pattern. The required modulation amplitude curves predicted by the fluctuation theory are not applicable at low spatial frequencies where the properties of the visual system limit modulation sensitivity. For 0.3 full moonlight plus clear night sky, the photoelectron emission rates

by the S25 and S20 VR cathodes are 2.46×10^5 and 5.59×10^5 photoelectrons/ $\text{mm}^2\text{-sec}$, respectively. For the clear night sky alone, the corresponding rates are 2.9×10^3 and 7.26×10^3 photoelectrons/ $\text{mm}^2\text{-sec}$, respectively. In all cases it was assumed that the numerical aperture of the objective is $f/2$ and that the reflectivity of the scene is 10 percent.

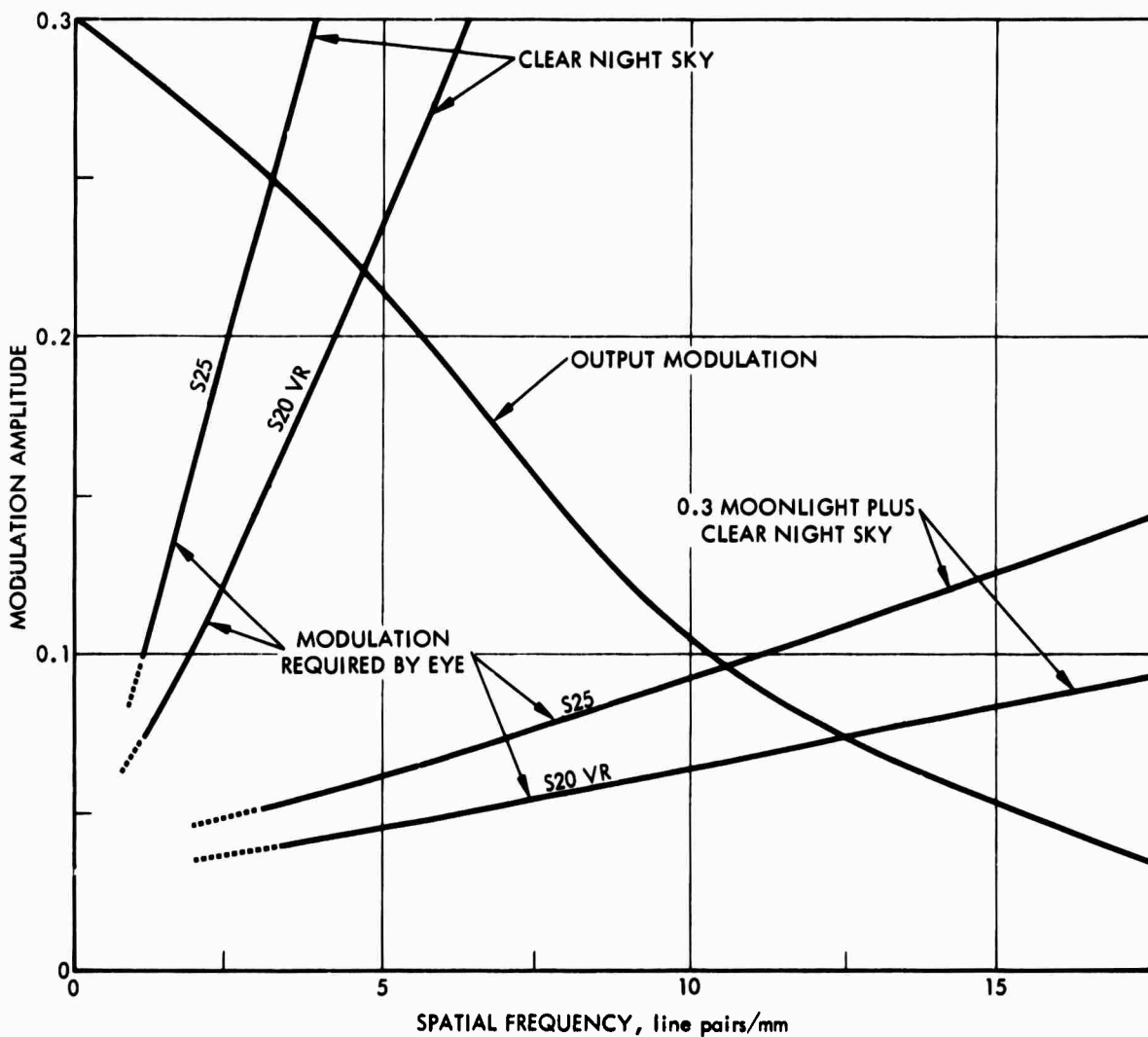


FIGURE 3. Passive Performance of Triple Image Intensifier.

Figure 3 displays two kinds of information about the performance of the triple image intensifier under the assumed conditions. First, the intersections of the required modulation amplitude curves with the output modulation amplitude curve for 30 percent input modulation determines the resolution for this specified input. Second, twice the

ratio of the output modulation to the required modulation at each value of the spatial frequency is equal to the S/N on the display.

In order to achieve the same performance with an active system, the required average laser power is given by

$$P = \pi F^2 \alpha^2 R^2 (h\nu_0) J / e \rho \eta(\lambda_0) \quad (15)$$

where the numerical aperture (F) of the image intensifier system objective is maintained at f/2, the average reflectivity (ρ) of the scene is 0.1, α is the angular divergence of the laser beam, R is the range to the target, J is the photocathode current density under either 0.3 full moonlight plus clear night sky or clear night sky alone, $h\nu_0$ is the energy of a laser photon and $\eta(\lambda_0)$ is the quantum efficiency of the photocathode at the laser wavelength (λ_0). A tabulation of the required average laser power for Ruby, cooled GaAs, and Nd^{3+} is given below:

		<u>Ruby</u>	<u>GaAs (Cooled)</u>	<u>Nd^{3+}</u>
Clear Night Sky (CNS)	{S25	0.0065 W	0.023 W	0.487 W (S1)
	{S20 VR	0.0065	0.018	1.22 (S1)
0.3 Moonlight Plus CNS	{S25	0.553	1.98	41.5 (S1)
	{S20 VR	0.504	1.36	94.5 (S1)

The average laser power values were calculated for a laser beam divergence of 0.05 radians or approximately 3 deg, $R \approx 1000$ m, and $\eta(\lambda_0)$ given in Section III. The appropriate quantum efficiencies of the S25 and S20 VR were chosen for calculation of ruby and cooled GaAs laser powers. However, only the S1 is available for detection of the Nd^{3+} laser power. A range of 1000 m was chosen since this represents a typical maximum detection range for a tank using a night observation device with an S25 photosurface and clear night sky illumination.

Some important conclusions concerning the relative importance of system parameters in both passive and active photoelectronic imaging systems are now apparent. Both result from the fact that because output modulation amplitude falls quickly with spatial frequency, the

resolution is quite insensitive to changes in photocathode current density either due to changes in quantum efficiency or input irradiance. For example, with input irradiance due to a clear night sky, the increase in resolution provided by the S20 VR compared to the S25 photocathode is from approximately 3.3 to 4.7 line pairs/mm--an increase of 42 percent for an increase in photoelectron emission rate of 150 percent. However, with input irradiance due to 0.3 moonlight plus clear night sky, the analogous increase is from 10.5 to 12.5 line pairs/mm--an increase of only 19 percent although the increase in photoelectron emission rate is 127 percent. The resolution of an ideal image intensifier with unity modulation transfer function at all spatial frequencies would increase in proportion to the square root of the photoelectric current density (i.e., as $\eta^{1/2}$). However, we see that due to the poor modulation transfer function of real image intensifiers, only a small part of the expected increase in performance can be realized. On the other hand, doubling the quantum efficiency in an active system will allow reduction of laser power by one-half to maintain the same performance.

A particularly significant example is the Nd^{3+} laser active system which at present utilizes the S1 photocathode with quantum efficiency of 0.00035. At 1000 m this system requires an average laser power of 94.5 watts to match passive operation of the S20 VR with 0.3 moonlight. However, there are indications that a factor-of-30 improvement in quantum efficiency for detecting the Nd^{3+} laser is in the offing, as discussed in Section III. Such an improvement would reduce the required average Nd^{3+} laser power to only 3 watts.

Another important conclusion is that if sufficient average laser power is available to provide an equivalent performance such as viewing a scene at 1000 m under 0.3 moonlight, then the same resolution will be maintained if the laser power is increased in proportion to the square of the range, as indicated in Eq. 15. Ideally, to detect a given target such as a tank, the resolution should be increased with range. Then if the modulation transfer function were ideal, the required laser power would increase as the fourth power of the range.

However, as shown in Fig. 3, the S20 VR under 0.3 moonlight comes close to providing the maximum resolution which aberrations allowed. Hence, even if additional power were available, it would not be possible to increase detection range beyond that of a passive system operating with 0.3 moonlight unless a system with a significantly improved modulation transfer function became available. However, the laser can provide the same operation under conditions of clear or overcast night sky as well as through obscuring atmosphere.

Consideration has been given to the use of the silicon vidicon as an image sensor, especially of the neodymium laser at 1.06μ where the quantum efficiency of photocathodes is low (0.035 percent for the S1). However, the silicon vidicon, like all vidicons, is limited in sensitivity by video preamplifier noise. The very best video preamplifiers exhibit noise-equivalent input currents of 2 to 3 namp in a 4-MHz bandwidth. This is equivalent to the signal received from a scene illuminated by five times full moonlight (5×10^{11} photons/cm²-sec) if it is assumed that the silicon target quantum efficiency is 20 percent, the f-number of the objective is 1.2, and the signal is great enough to provide the full resolution determined by video bandwidth of ~ 500 television lines. On the other hand, the thermionic current of an uncooled S1 photocathode is about 10^{-12} amp/cm², which for an objective lens f-number of 1.2 and a quantum efficiency of 0.035 percent is equivalent to the signal received from a scene illuminated by $\sim 1.5 \times 10^{11}$ photons/cm²-sec. Thus, the uncooled S1 photocathode is somewhat more sensitive than the silicon vidicon. With cooling to -20°C the S1 dark current is reduced by a factor of 1000, whereas the video preamplifier noise of the vidicon remains essentially unchanged. Clearly the S1 photocathode is far superior to the silicon vidicon where high sensitivity is required. Of course, the S1 photocathode must be incorporated as the image sensor in an image intensifier preamplifier to utilize greater sensitivity. Other photocathodes under development which show promise of achieving greatly improved quantum efficiencies (as high as 1 percent at 1.06μ), such as the ternary III-V compounds treated with cesium oxide, are discussed in detail in Section III. Other silicon vidicon configurations such as the return beam and isocon readout designed to achieve greater sensitivity than the conventional vidicon

readout suffer from increased electron lag caused by the time constant of target capacitance and beam-charging current. This problem is particularly aggravated by the high capacitance (several thousand pf) of the silicon array compared with the low capacitance (several tens) of pf) of the SEC vidicon, orthicon, and plumbicon targets.

The silicon vidicon may find application as a rugged and less expensive primary sensor when light is abundant. However, it will not be able to compare with improved photocathodes when photons are scarce. This, of course, does not mean that it cannot be used as a storage target after a photocathode image intensifier, but such use is primarily an engineering problem. The ultimate sensitivity will be limited by the primary photocathode. Nothing special to laser applications is involved in this use of the silicon diode array vidicon.

XI. RECOMMENDATIONS

A. DEVELOPMENT OF III-V SEMICONDUCTORS

It is strongly recommended that a substantial program be undertaken for the development of III-V semiconductor alloys that have variable energy gaps in the 0.5- to 1.2-ev range, i.e., $\text{InAs}_{1-x}\text{P}_x$, $\text{In}_{1-x}\text{Ga}_x\text{As}$, and $\text{GaAs}_{1-x}\text{Sb}_x$.

1. Primary Objective

The main objective of such a program would be to support the development of a photoemitter of 1 percent quantum efficiency for 1.06μ . Epitaxially grown single-crystal films that have $E_g \sim 1.1$ ev (and $t < 1\mu$ for imaging systems) and the electrical properties of sharp band bending, high electron mobility, and long carrier lifetime in the transverse direction are needed. Work on these materials must be combined with work on a photoemission device, since at present the only way to evaluate a film is to make a photocathode that incorporates the film. The development of other techniques to measure the quality of materials would be very useful. Material growth and cathode manufacture in the same vacuum have not been tried but might have

advantages. Reflection mode devices will come first but semitransparent photocathodes should be the ultimate goal.

2. Secondary Objectives

Other objectives of the development of such materials would be:

- To support efforts to develop photocathodes for 1.5μ to 1.7μ , $E_g \sim 0.7$ to 0.8 ev; and 2.1μ , $E_g \sim 0.5$ ev.
- To provide the technological base for diode and avalanche diode development for 1.65μ and 2.1μ .

B. OPTIMIZATION OF III-V PHOTOCATHODES

Device research to understand and optimize new photocathodes should also be supported. This research should involve:

1. High-priority work on heterojunction cathodes, to include for 1.06μ :
 - Optimizing p-type doping and surface layer thickness
 - Understanding the effect of the heterojunction potential spike
 - Trying new surface materials and treatments
 - Identifying possible new contaminants
 - Understanding the origin of electron thermionic emission
 - Finding an n-type surface layer material of lower electron affinity (specially important for $\lambda \geq 1.5\mu$)
2. Work on biased-surface cathodes for $\lambda \geq 1.5\mu$.

For 1.06μ heterojunction cathodes, it is not too soon to think about developing a production capability. This would involve:

- Learning how to seal them off in a useful tube
- Life testing

For detectors for eye-safe wavelengths, a variety of higher-risk programs will be necessary.

C. INTERNAL PHOTOEFFECT DETECTORS FOR $\lambda \geq 1.5\mu$

Work with avalanche diodes will be important for $\lambda \geq 1.5\mu$, although at the moment no particular program can be given a high priority. Schottky barrier avalanche techniques might marginally extend the useful wavelengths of germanium avalanche diodes. Ion implantation techniques could improve yields and allow larger diodes. Work to make avalanche diodes from InAs should be supported, especially if a 2.1μ laser is to be developed.

If the materials technology for the previously mentioned III-V semiconductor alloys is developed, avalanche diodes from these materials would be very useful, especially for 1.65μ , and should eventually receive high priority. Diodes made from $\text{Hg}_{1-x}\text{Cd}_x\text{Te}$ are an alternative.

The progress of ac bias techniques should be monitored, especially as regards lower-noise microwave components and the possible appearance of a photoconductive material suitable for high-performance ac bias detection at 1.65μ ($T > 260^\circ\text{K}$).

The development of large-area ($\sim 1 \text{ cm}^2$) photodiode quadrants made from III-V semiconductor alloys for 1.65μ detection should receive high priority.

XII. OVERVIEW: DETECTORS FOR LASER APPLICATIONS

If military laser systems continue to use 1.06μ , the detection problem is clear. The development of a surface of 1 percent quantum efficiency will make all other detectors at 1.06μ obsolete except possibly PIN silicon quadrants. The advantages of covertness at 1.06μ can then be well utilized. The difference in detection sensitivity for small-area point detectors (rangefinders) between 1.06μ and 0.53μ will go approximately as $[\eta_1^{1/2} \lambda_1]/[\eta_2^{1/2} \lambda_2] = 3$ for sunlit backgrounds and as $\eta_1 \lambda_1 / \eta_2 \lambda_2 = 15$ at night.

New photocathodes probably will not bring improvements for target-designator systems for daytime operation.

Imaging system improvements at 1.06μ will, however, benefit most from new semitransparent photosurfaces. Laser power requirements at 1.06μ should be reduced by a factor of $\eta_1/\eta_2 \sim 1/30$. Imaging systems at 0.53μ will then be more sensitive by only a factor of 10 to 100 if cooling of the photocathode is allowed. This is much less a difference than at present. Thus, ruby and doubled YAG will be less important. Photocathode improvement at 1.06μ does not, of course, provide a sensitive infrared film for those applications requiring maximum resolution. Thus for certain applications visible radiation will still be required.

The problem of the target designator is an intriguing one. The quadrant detector tends to be easily background limited so that improvements can only come from improved filters and signal processing. The 10-pps requirement on the laser comes from a desire for a single high-peak-power pulse per servo integration time to accommodate the square law detector. Shorter servo integration times for advanced systems might have slightly higher repetition rates. The most straightforward analysis suggests that a system having a repetition rate higher than required with N pulses (of the original pulse width) per integration time would need at least a factor of \sqrt{N} more average power to achieve the same detection performance.

This issue is important since 10 pulses/sec (pps) is not necessarily the most natural laser pulse repetition rate.

Possibly the easiest way to obtain high average power Q-switched is to provide continuous pumping with Nd^{3+} YAG and to Q-switch at the inverse fluorescent lifetime (200 μsec with Nd^{3+} in YAG), i.e., at 5 kHz. It has been claimed that several special pumping schemes that require relatively cool lamp operation for efficient performance could possibly provide greater efficiency operating cw than a repetitively pumped (10 pps) laser of the same average power. Even if the cw-pumped laser were five times as efficient, this would not make up for the 10 to 100 reduction in detection performance. Mode-locked lasers produce picosecond pulses with a repetition frequency in the 3-GHz range. This

repetition rate is much too high for target designators, and, unfortunately, no target designators are as yet available that can resolve a picosecond pulse in such a way as to take advantage of its high peak power. There is good reason for the 10-pps requirement for the designator. These considerations do not hold for the illuminator. As long as proper gating is provided, pulse rates greater than 30 pps would do just as well.

The prognosis for detector improvements for eye-safe wavelengths ($\lambda > 1.5\mu$) is much less clear. Germanium avalanche diodes can operate moderately well at 1.54μ if they are cooled and large-area germanium PIN diodes can operate cooled at 1.65μ . So the tendency will be to use Er^{3+} doped glass (1.54μ) systems for low-repetition-rate range-finders and (unless a Raman laser or a segmented glass technology is developed) Er^{3+} doped YAG (1.65μ) for the high-average-power target designator.

Er^{3+} doped YAG could possibly make a more efficient rangefinder, but a convenient high-gain detector for 1.65μ has yet to be realized. Combination rangefinder/target-designator systems need only a high-performance rangefinder detector if the laser operates in a dual mode with lower-energy rangefinder pulses to conserve battery power. Otherwise, the large pulse energies needed for the target designator (with its background-limited quadrant) are more than enough for quite a simple detector for the rangefinder.

If eye-safe wavelengths are judged to be important, a long-range program must be pursued to explore a variety of high-risk approaches.

REFERENCES

1. L. K. Anderson, M. DiDomenico, and M. B. Fisher, High Speed Photodetectors for Microwave Demodulation of Light, to be published.
2. Electro-Optics Handbook, RCA Defense Electronic Products, Aerospace Systems Division, Burlington, Mass., 1965.
3. Institute for Defense Analyses, Close Air Support Weapons, L. M. Biberman, J. A. Navarro, R. E. Schwartz, and J. G. Taylor, IDA Research Paper P-479, May 1969.
4. L. K. Anderson and B. J. McMurtry, "High Speed Photodetectors," Appl. Opt., Vol. 5, pp. 1573-1587, 1966.
5. J. J. Uebbing and R. I. Bell, "Improved Photoemitters Using GaAs and InGaAs," Proc. IEEE, Vol. 56, p. 1624, 1968.
6. J. J. Uebbing, Varian Associates, private communication, 1969.
7. J. van Laar and J. J. Scheer, "Photoemission of Semiconductors," Philips Tech. Rev., Vol. 29, pp. 54-66, 1968.
8. H. Sonnenberg, "Low-Work Function Surfaces for Negative-Electron Affinity Photoemitters," Appl. Phys. Letters, Vol. 14, pp. 289-291, 1969.
9. J. J. Uebbing and L. W. James, "The Behavior of Cesium Oxide as a Low-Work Function Coating," Conference on Photoelectric and Secondary Electron Emission, University of Minnesota, August 27 and 28, 1969.
10. C. Hilsum and A. C. Rose-Innes, eds., Semiconducting III-V Compounds, Pergamon Press, London, 1961.
11. Varian Associates, Central Research Laboratories, 1.06 Micron Image Converter, R. Bell et al., AFAL-TR-69-162, prepared for Air Force Avionics Laboratory, Wright-Patterson AFB, Ohio, April 1969.
12. E. D. Savoye, Radio Corporation of America, Princeton, N.J., private communication, 1969.
- 12a. H. Sonnenberg, "InAsP-Cs₂O, A High-Efficiency Infrared-Photocathode," Appl. Phys. Letters, Vol. 16, No. 6, 15 March 1970.

13. W. Klein, "Photoemission from Cesium Oxide Covered GaInAs," J. Appl. Phys., Vol. 40, pp. 4384-4389, 1969.
14. Brown F. Williams, "InGaAs-CsO, a Low-Work Function (less than 1.0 ev) Photoemitter," Appl. Phys. Letters, Vol. 14, No. 9, pp. 273-275, 1969.
15. S. S. Perlman and D. L. Feucht, "P-N Heterojunctions," Solid-State Electronics, Vol. 7, pp. 911-923, 1964.
16. Minoru Hagino and Ryoza Nishida, "Photoemission from GaAs-Cs-Sb (Te)," Japan. J. Appl. Phys., Vol. 8, p. 123, 1969.
17. K. Miyaji, Report No. J-255-3, Contract DA-92-557-FEC-38337.
18. R. E. Simon and W. E. Spicer, Phys. Rev., Vol. 119, p. 621, 1960.
19. P. R. Thornton and D. C. Northrop, Solid State Elect., Vol. 8, p. 437, 1965.
20. R. E. Simon and W. E. Spicer, "Field Induced Photoemission and Hot-Electron Emission from Germanium," J. Appl. Phys., Vol. 31, p. 1505, 1960.
21. I. G. Davies and P. R. Thornton, Appl. Phys. Letters, Vol. 10, p. 249, 1967.
22. C. Thomas, "IR Controlled Tunnel Emitter," presented at 16th Nat. IRIS Meeting, May 1968.
23. E. D. Savoye, Infrared Photoemission from SiAl₂O₃-GaP-Cs Structures, Conference on Photoelectric and Secondary Electron Emission, University of Minnesota, August 27 and 28, 1969.
24. R. E. Simon, A. H. Sommer, J. J. Tietjen, and B. F. Williams, "New High-Gain Dynode for Photomultipliers," Appl. Phys. Letters, Vol. 13, pp. 355-356, 1968.
25. R. J. McIntyre, "Multiplication Noise in Uniform Avalanche Diodes," IEEE Trans. on Electron Devices, Vol. 13, pp. 164-168, 1966.
26. H. Melchior and W. T. Lynch, "Signal and Noise Response of High Speed Germanium Avalanche Photodiodes," IEEE Trans. on Electron Devices, Vol. 13, pp. 829-838, 1966.
27. Texas Instruments, Inc., Broadband Optical Detectors (1.06 Micron), W. N. Shaunfield, Technical Report ECOM-02379-F, prepared for U.S. Army Electronics Command, Ft. Monmouth, N.J., August 1967.
28. W. N. Shaunfield, Texas Instruments, Inc., private communication, 1969.

29. RCA Victor Company, Ltd., Research Laboratories, A New Germanium Photodiode with Extended Long-Wavelength Response, R. J. McIntyre, E. P. Mathur, and P. P. Webb, Research Memorandum 249, File No. 72.16.3, 1968.
30. A. Frova et al., "Electro-Absorption Effects at Band Edges of Silicon and Germanium," Phys. Rev., p. 575, 1966.
31. W. T. Lindley, R. J. Phelan, C. M. Wolfe, and A. G. Foyt, "GaAs Schottky Barrier Avalanche Photodiodes," Appl. Phys. Letters, Vol. 14, pp. 197-199, 1969.
32. Lloyd DeVaux, Hughes Aircraft Company, Malibu, Calif., private communication, 1969.
33. G. S. Picus, "Infrared Detectors for Laser Systems," IEEE Conference on Laser Engineering and Applications, May 26-28, 1969, Digest of Technical Papers, IEEE Catalog No. 69C27-LASER, p. 14.
34. M. Rome, H. G. Fleck, and D. C. Hines, "The Quadrant Multiplier Phototube, a New Star-Tracker Sensor," Appl. Opt., Vol. 3, p. 691, 1964.
35. Alan N. Kohn and J. J. Schlickman, "1-2 Micron (Hg, Cd) Te Photo-detectors," IEEE Trans. on Electron Devices, Vol. ED-16, p. 885, 1969.
36. J. J. Schlickman, Honeywell Radiation Center, Lexington, Mass., private communication.
37. H. S. Somers and E. K. Gatchell, "Demodulation of Low-Level Broad-band Optical Signals with Semiconductors," Proc. IEEE, Vol. 54, pp. 1553-1568, 1966.
38. G. Biernson and R. F. Lucy, "Requirements of a Coherent Laser Pulse-Doppler Radar," Proc. IEEE, Vol. 51, pp. 202-213, 1963.
39. G. C. Holst and E. Snitzer, "Detection with a Fiber Laser Pre-amplifier at 1.06μ ," IEEE Conference on Laser Engineering and Applications, May 26-28, 1969, Digest of Technical Papers, IEEE Catalog No. 69C27-LASER, p. 13.
40. J. E. Midwinter and J. Warner, "Up-Conversion of Near Infrared to Visible Radiation in LiNbO_3 ," J. Appl. Phys., Vol. 38, p. 519, 1967.
41. A. H. Firester, Radio Corporation of America, Princeton, N.J., private communication, 1969.
42. J. Falk and J. Murray, "Single-Cavity Noncollinear Optical Parametric Oscillation," Appl. Phys. Letters, Vol. 14, p. 245, 1969.

43. N. Bloembergen, "Solid State Infrared Quantum Counters," Phys. Rev. Letters, Vol. 2, p. 84, 1959.
44. A. Rose, J. Opt. Soc. Am., Vol. 38, p. 196, 1948.
45. John W. Coltman, J. Opt. Soc. Am., Vol. 44, p. 234, 1954.
46. J. W. Coltman and A. E. Anderson, Proc. IRE, Vol. 46, p. 858, 1960.
47. O. H. Schade, Sr., RCA Review, Vol. 28, p. 460, 1967.

UNCLASSIFIED

Security Classification

DOCUMENT CONTROL DATA - R & D

(Security classification of title, body of abstract and indexing annotation must be entered when the overall report is classified)

1. ORIGINATING ACTIVITY (Corporate author) INSTITUTE FOR DEFENSE ANALYSES 400 Army-Navy Drive Arlington, Virginia 22202		2a. REPORT SECURITY CLASSIFICATION UNCLASSIFIED	
		2b. GROUP --	
7. REPORT TITLE Detection Considerations for Laser Systems in the Near Infrared: Prognosis for an Improved Technology			
8. DESCRIPTIVE NOTES (Type of report and inclusive dates) Research Paper P-581, April 1970			
3. AUTHOR(S) (First name, middle initial, last name) A. Fenner Milton Alvin D. Schnitzler			
9. REPORT DATE April 1970	7a. TOTAL NO. OF PAGES 51	7b. NO. OF REFS 48	
5a. CONTRACT OR GRANT NO. DAHC15 67 C 0011 b. PROJECT NO. ARPA Assignment 5 c. d.		6a. ORIGINATOR'S REPORT NUMBER(S) P-581 6b. OTHER REPORT NO(S) (Any other numbers that may be assigned this report) None	
10. DISTRIBUTION STATEMENT This document has been approved for public release and sale; its distribution is unlimited.			
11. SUPPLEMENTARY NOTES NA		12. SPONSORING MILITARY ACTIVITY Advanced Research Projects Agency Washington, D.C.	
11. ABSTRACT This paper summarizes the influence of detection considera- tions on the standard military optically pumped laser systems. The problems and uncertainties associated with the development of new photocathodes for the near infrared are discussed in detail. A variety of laser detection schemes are examined to determine their potential in the $\lambda = 1.5\mu$ to 2.5μ region. The problems of imaging systems for use with laser illuminators are discussed. A research program is recommended to improve detector performance.			

14	KEY WORDS	LINK A		LINK B		LINK C	
		ROLE	WT	ROLE	WT	ROLE	WT